

# **Final Report**

**High resolution (1.33 km) MM5 modeling of the  
September 1993 COAST episode: Sensitivity to model  
configuration and performance optimization.**

**Work Assignment Number 31984-18  
TNRCC Umbrella Contract Number 582-0-31984**

Prepared for:

**Texas Natural Resource Conservation Commission  
12118 Park 35 Circle  
Austin, Texas 78753**

Prepared by:

**ENVIRON International Corporation  
101 Rowland Way, Suite 220  
Novato, California 94945**

**ATMET, LLC  
PO Box 19195  
Boulder, Colorado 80308-9195**

**15 February 2002**

## Table of Contents

1.	<a href="#">Introduction</a>	1
2.	<a href="#">MM5 Description</a>	2
3.	<a href="#">MM5 Grid Structure</a>	3
4.	<a href="#">Input data access and preparation</a>	4
4.1.	<a href="#">Atmospheric data</a>	4
4.2.	<a href="#">Terrain Data</a>	5
5.	<a href="#">Model physics configuration</a>	6
6.	<a href="#">Statistical methodology and output files</a>	8
7.	<a href="#">Sensitivity Simulations</a>	9
7.1.	<a href="#">Introduction</a>	9
7.2.	<a href="#">Control Simulations</a>	11
7.3.	<a href="#">PBL Tests</a>	13
7.3.1.	<a href="#">Two-grid PBL tests</a>	13
7.3.2.	<a href="#">Three-grid PBL tests</a>	19
7.3.3.	<a href="#">Shallow convection tests</a>	28
7.3.4.	<a href="#">MRF PBL tests</a>	28
7.3.5.	<a href="#">Gayno-Seaman PBL tests</a>	30
7.4.	<a href="#">Microphysics tests</a>	33
7.5.	<a href="#">FDDA nudging effect test</a>	35
7.6.	<a href="#">Discussion of Sensitivity Results</a>	41
7.6.1.	<a href="#">Underprediction of surface wind speed</a>	41
7.6.2.	<a href="#">Lack of sea breeze circulations</a>	41
7.6.3.	<a href="#">Convective cells</a>	43
8.	<a href="#">New 4 grid simulations</a>	46
9.	<a href="#">Summary</a>	58

# 1. Introduction

A previous set of meteorological simulations was performed under the project: MM5/RAMS Fine Grid Meteorological Modeling for September 8-11, 1993 Ozone Episode, Work Assignment Number 31984-12, TNRC Umbrella Contract Number 582-0-31984. The RAMS and MM5 simulations were performed for the period 6-11 September 1993 for the Houston/Galveston region. MM5 was run in both a 3-grid configuration (with 4 km finest grid) and a 4-grid configuration (1.33 km finest grid). Although the statistical verification results of MM5 were acceptable, during the examination of the MM5 meteorological fields, several undesirable features were apparent. The most notable of these features were:

- Consistent underprediction of the sea breeze development
- Underprediction of surface wind speeds over land during the day
- Creation of explicit, grid-scale thunderstorms which generated very strong outflows. These outflows were so strong at times that the low-level wind field was completely disrupted.

These features are not unique to this set of MM5 runs - other MM5 users have reported these to one degree or another. The tight schedule for the previous project did not allow enough time to perform the number of sensitivity tests required to determine which of the various MM5 physical parameterizations that were used caused these problems. We anticipated that the likely causes of these features center on:

- The sea-breeze underprediction may be caused by the MM5 default soil moisture content that was too high. This is borne out by the statistical results which showed that there was generally a high moisture bias in the MM5 results, although there was not a consistent low temperature bias.
- The underprediction of surface wind speeds over land may be caused by the surface layer schemes extracting too much momentum from the air, or by the PBL scheme mixing momentum too rapidly in the vertical. These schemes also play a role in the sea breeze development.
- The erroneous convective development may be caused by the explicit moisture schemes. While we tried two different explicit moisture schemes in the 3 and 4 grid runs with the same results, there are other options in MM5 that could be tried. The PBL scheme could also be at fault here, as it may have mixed moisture too high in the atmosphere, which triggered the condensation and convection.
- Interaction of FDDA with the aforementioned schemes might play a role in some of these features by, for example, maintaining convergence zones.

The purpose of this work assignment is to investigate which MM5 parameterizations are responsible for the undesirable features, make adjustment to the model configuration to compensate, and to produce new meteorological fields for the 6-11 September 1993 episode using MM5 with the configuration decided from the results of the sensitivity simulations.

The following sections will detail the various sensitivity tests that we performed, our reasons for selecting the new MM5 configuration, and present the verification from the full episode simulation. We repeat some of the model and data configuration details from the previous projects for completeness. While some of our predictions of the causes of the undesirable features were correct, other unexpected factors came into play.

## 2. MM5 Description

The Fifth-Generation NCAR / Penn State Mesoscale Model (MM5) is the latest in a series that developed from a mesoscale model used by Anthes at Penn State in the early 70's that was later documented by Anthes and Warner (1978). Since that time, it has undergone many changes designed to broaden its usage. These include (i) a multiple-nest capability, (ii) nonhydrostatic dynamics, which allows the model to be used at a few-kilometer scale, (iii) multitasking capability on shared- and distributed-memory machines, (iv) a four-dimensional data-assimilation. MM5 uses a terrain-following  $\sigma_p$ -coordinate model designed to simulate or predict mesoscale and regional-scale atmospheric circulations. Sigma surfaces near the ground closely follow the terrain, and the higher-level sigma surfaces tend to approximate isobaric surfaces. The physics options available in the latest release of MM5 (3-5) include:

- Cumulus parameterization schemes:
  - Anthes-Kuo
  - Grell
  - Kain-Fritsch
  - New Kain-Fritsch (including shallow convection physics)
  - Betts-Miller
  - Arakawa-Schubert
- Resolvable-scale microphysics schemes:
  - Removal of supersaturation
  - Hsie's warm rain scheme
  - Dudhia's simple ice scheme
  - Reisner's mixed-phase scheme
  - Reisner's mixed-phase scheme with graupel
  - NASA/Goddard microphysics with hail/graupel
  - Schultz mixed-phase scheme with graupel
- Planetary boundary layer process parameterization
  - Bulk formula
  - Blackadar scheme
  - Burk-Thompson (Mellor-Yamada 1.5-order/level-2.5 scheme)
  - ETA scheme (Janjic, 1990, 1994)
  - MRF scheme (Hong and Pan 1996)
  - Gayno-Seaman scheme (Gayno 1994)
- Surface layer process parameterization
  - fluxes of momentum, sensible and latent heat
  - ground temperature prediction using energy balance equation
  - variable land use categories (defaults are 13, 16 and 24)
  - 5-layer soil model
  - OSU land-surface model (V3 only)
  - Pleim-Xiu land-surface model (V3 only)

- Atmospheric radiation schemes
  - Simple cooling
  - Dudhia's long- and short-wave radiation scheme
  - NCAR/CCM2 radiation scheme
  - RRTM long-wave radiation scheme (Mlawer et al., 1997) (V3 only)

### 3. MM5 Grid Structure

For the simulations of 6-11 September 1993, MM5 was configured with the same grid structure as in the previous project. Table 1 summarizes the MM5 grid configuration and Figure 1 depicts the MM5 horizontal grid structure.

**Table 1 : MM5 grid configuration for the Houston/Galveston runs.**

Grid	# of X points	# of Y Points	Vertical Levels	$\Delta x$ (km)	$\Delta y$ (km)	$\Delta z$ (m) (Lowest)
1	72	66	41	36	36	10
2	139	124	41	12	12	10
3	139	118	41	4	4	10
4	127	118	41	1.33	1.33	10

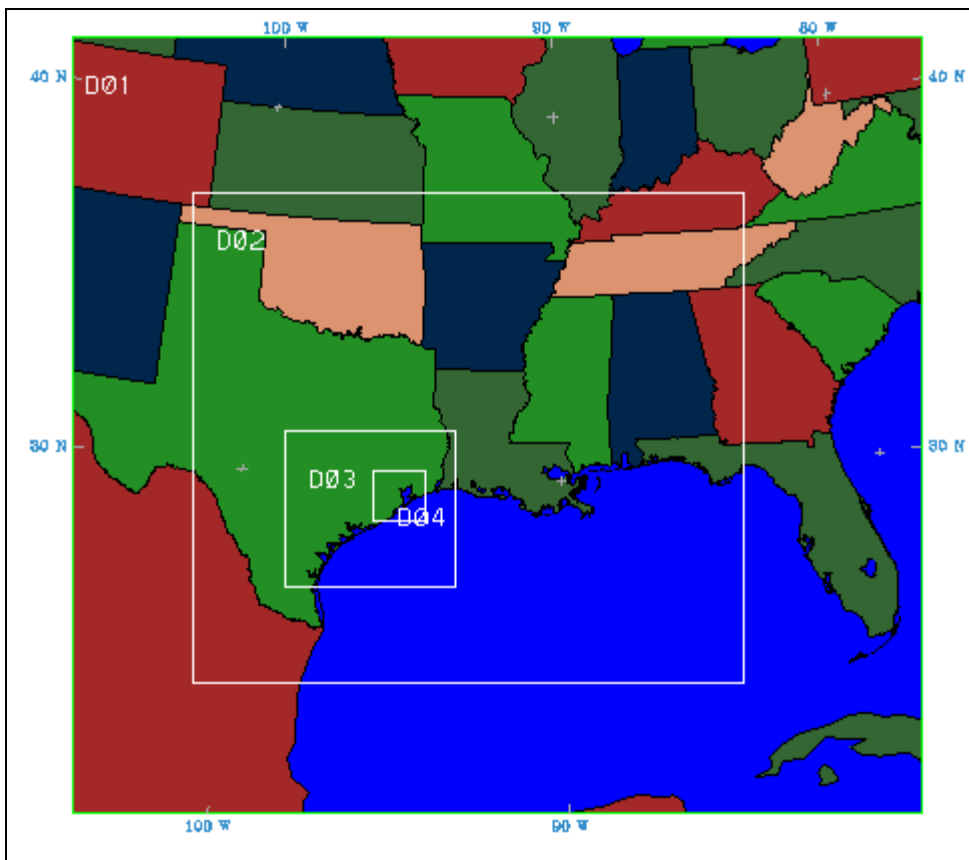


**Figure 1 : MM5 grid configuration for the 4-grid run.**

In the vertical, MM5 had the same grid structure as the previous project, which was configured to match the previous project’s RAMS vertical levels as closely as possible. This was somewhat more difficult to do, since MM5 is a terrain-following pressure coordinate, rather than terrain-following height like RAMS and CAMx. We chose to configure MM5 with the  $\sigma_p$  levels shown in Table 2: 41  $\sigma_p$  levels (40 layers) with the top pressure of 50 mb.

**Table 2 : MM5 vertical sigma-p layer interfaces.**

1.000	0.998	0.995	0.990	0.985	0.980	0.975	0.965
0.955	0.940	0.925	0.910	0.895	0.875	0.855	0.835
0.810	0.785	0.755	0.725	0.695	0.660	0.625	0.590
0.540	0.485	0.425	0.360	0.300	0.250	0.200	0.160
0.125	0.100	0.075	0.050	0.035	0.025	0.015	0.010
0.000							

These sigma levels were determined by converting the RAMS height levels to equivalent pressure levels by assuming a hydrostatic base state of:

- surface pressure of 1000mb
- model top at 50mb
- surface temperature of 295K
- lapse rate of 50K/lnP (roughly 6.5K/km)

Using this base state, and the hydrostatic relation, one can cast the  $\sigma_p$  equation:

$$\sigma_p = \frac{(p - p_{top})}{(p_{sfc} - p_{top})}$$

in terms of the base state and Cartesian height. The  $\sigma_p$  levels used were computed from the RAMS sigma-z heights.

## 4. Input data access and preparation

### 4.1. Atmospheric data

For these simulations, we used the same input data as used on the previous projects. The meteorological input data to the meteorological models can be grouped into three categories:

1. **Large scale gridded analyses:** Global analyses of meteorology are available from the National Centers for Environmental Prediction (NCEP). We used the NCEP/NCAR Reanalysis data. The parameters of wind, temperature, and humidity are analyzed on pressure levels (20 levels extending from 1000 mb up to 10 mb) on a 2.5 degree latitude-longitude grid. These data are archived every 6 hours and serve as a first guess field for the data analysis. We accessed this data from the National Center for Atmospheric Research (NCAR).
2. **Standard NWS observations:** The rawinsondes and surface observations reported by the NWS and other national meteorological centers are also archived

at NCAR. The rawinsondes are reported every 6 hours and the surface observations are archived every three hours. These data were accessed for the 6 day period.

3. **Special observations from the COAST/GMAQS monitoring sites:** Special observations taken in August/September 1993 from the GMAQS/COAST monitoring sites were included in the data analyses and FDDA. These observations included surface observations, wind profilers, and a rawinsonde. However, on the previous projects, upon investigation it appeared that virtually all of the wind profilers and the rawinsonde were no longer available by the September episode. Therefore, we used only the available surface observations.

On the previous projects, all NCAR and COAST observational data were processed with our quality control algorithms. We have developed a QC package which consists of three separate schemes: 1) internal consistency checks, 2) “buddy” checks, and 3) “first-guess field” checks. The internal consistency checks consist of basic sanity and range checking of the observational data along with the physical constraints of hydrostatic balance. The buddy checks will compare a station’s value with that of its neighboring stations. The checks versus the first-guess fields will compare an observation against the large-scale gridded pressure data analyses. At any of these three stages, observational data values can be flagged as missing, bad, suspect, or corrected.

#### **4.2. Terrain Data**

The terrain data used on grids 3 and 4 (4 km and 1.33 km grid spacings) in these simulations originated from 30 second USGS data. The terrain data used on grids 1 and 2 (36 km and 12 km grid spacings) in these simulations originated from the 2 minute USGS data (30 second data averaged to the 2 minute scale). Vegetation/landuse fields also originated from the 2 minute and 30 second USGS data. The dominant landuse category is chosen for each model grid point.

Initial, boundary and nudging data are a combination of gridded analysis from the NCEP reanalysis project blended with surface and upper air observations. The reanalysis gridded fields are available at 2.5 degree horizontal resolution and time resolution of 6 hours. Upper air observations were obtained from the NCAR ADP archive which has a twelve hour time frequency. Surface observations were also obtained from the NCAR ADP archive and are available at 3 hourly intervals. The special COAST surface observations were also used at a 3 hourly frequency.

MM5 used its own data analysis package for its input data analysis. Options include a multi-pass Cressman analysis as well as a multiquadric analysis. The Cressman analysis was used in the previous work while the multiquadric analysis option was used in the current work, based on past experience with it. The analyses occur on pressure levels and a variety of quality control tests are performed to remove spikes from temperature and wind profiles and to remove superadiabatic layers. In addition, the observations are checked for consistency with the first guess gridded fields.

## 5. Model physics configuration

For the previous project, we attempted to configure MM5 physics to approximate the RAMS configuration as closely as possible, given the choice of MM5 schemes. Following is a summary of the model options used on the previous project:

- Grell convective parameterization
- Gayno-Seaman PBL scheme
- Mixed-Phase Reisner scheme for the 3-grid run, Schulz microphysics for the 4-grid run.
- The Cloud-Radiation scheme.
- Analysis (Grid) nudging was used for four-dimensional data assimilation (FDDA). Both the surface and upper air nudging was used. Nudging fields were available every 6 hours for upper air fields and 3 hourly for surface fields.

For the current set of runs, along with the numerous sensitivity tests, various changes were made to the basic configuration based on our experience. These are:

- MM5 version 3-5 was used for these simulations; MM5 version 3-4 was used in the previous work.
- The sea surface temperature (SST) for all simulations in this project was obtained from the Reynolds et al. monthly climatology available from NCAR/SCD (ds277.0). This climatology has global analyses with a 1 degree resolution available for each month since November 1981 (the data for September 1993 were used in this case). An OI scheme is used to blend marine surface observations and satellite AVHRR data. The previous simulation estimated the SST from the pressure-level atmospheric data set. The two different SST analyses are shown in Figure 2. The SST in the new simulations is about 1C cooler than that in the previous simulation.
- A simple "bucket" soil moisture scheme was included in most of the new simulations. This option allows the soil to moisten from precipitation and dry through evaporation and runoff. The initial soil moisture was estimated using the default option - it is simply based on the climatology associated with that land use type. The previous simulation was initialized with that same default climatology soil moisture assumption - the difference in that run is that the soil moisture never varies from the initial point onwards. The soil moisture over the domain is relatively dry in both cases although the inclusion of the bucket option does allow it to moisten where significant precipitation occurs. Figure 3 shows the default initialization soil moisture availability over grid 2 and then the same field after 24 hrs. If the bucket soil moisture scheme is not used (as in the original simulations), then the soil moisture stays the same as the default initialization throughout the integration.
- A slightly longer timestep was used in the new simulations (108 vs. 90 seconds on the coarse grid).
- The cumulus parameterization scheme was changed to the Kain-Fritsch scheme from the Grell scheme for most simulations, based on past experience that the Grell scheme seems to result in an over-development of the grid-scale

convection on smaller scales and in moister regimes. Also, the cumulus parameterization was turned on for both grids 1 and 2 (36 and 12 km grid spacing) in the new simulations while it was only used on grid 1 in the original simulations.

- All analyses, FDDA input files, and model input files were re-generated from the first-guess and observations files. This was done primarily as a consistency check but was also necessary because of a slightly different terrain specification. The data input files (first guess and observation) were the same as used in the previous experiment. The analysis was changed to the multiquadric option in the MM5 RAWINS package from the Cressman banana scheme option used in the previous work. The multiquadric scheme was chosen on the basis of past positive experience with it.

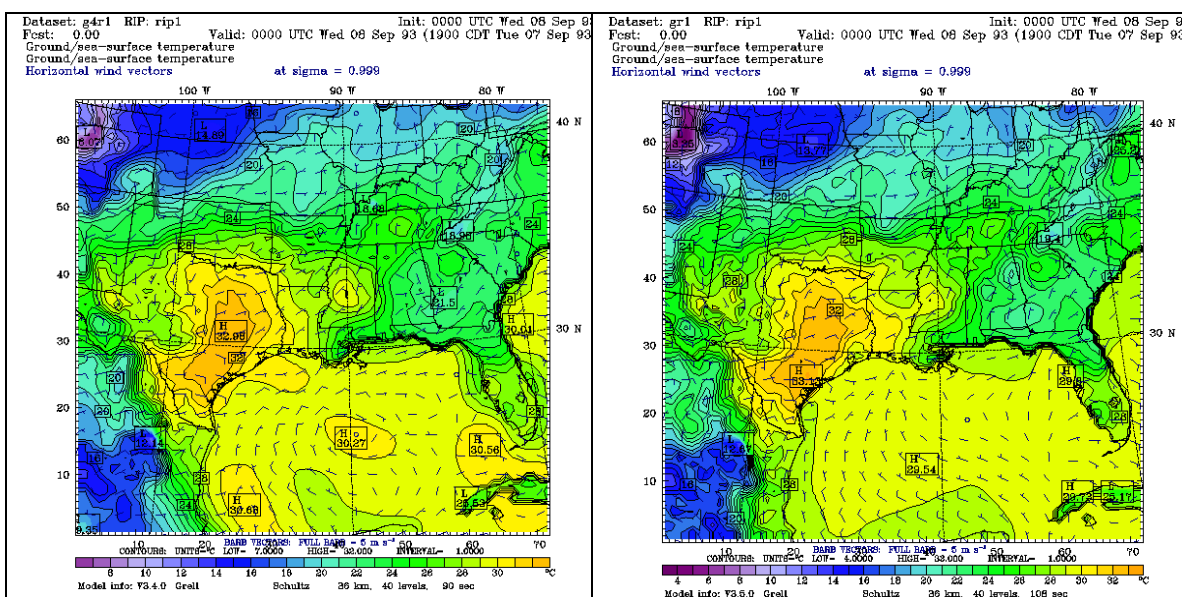
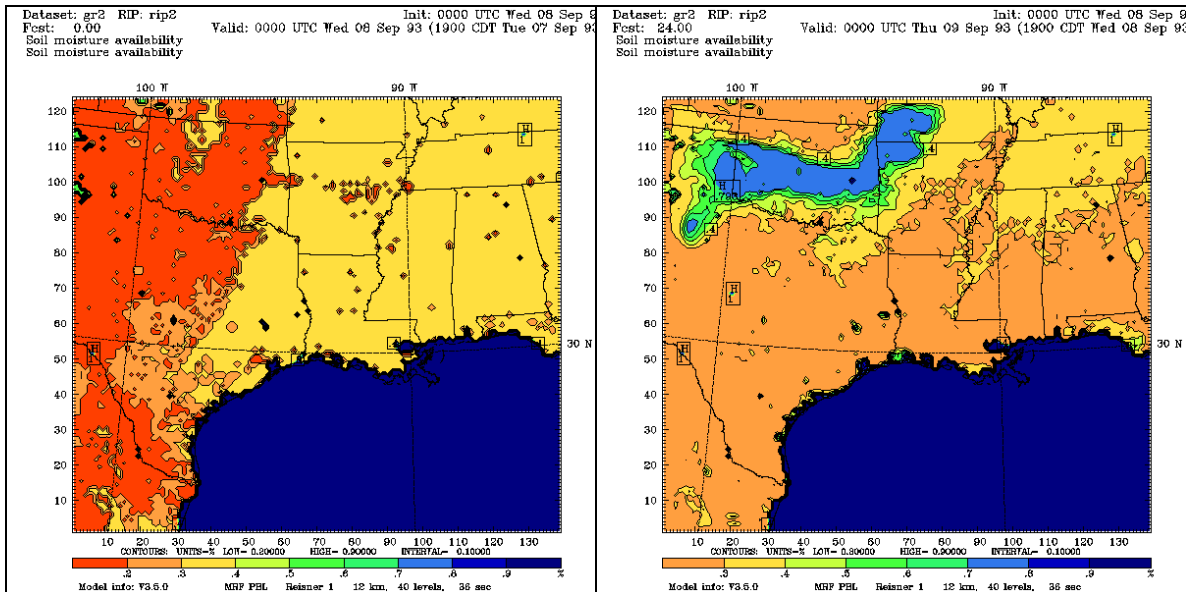


Figure 2 : Analysis at 00 UTC 8 Sept 1993 of ground temperature and SST over the grid 1 domain for a) Runorig4 and b) all new simulations.



**Figure 3 : Soil moisture availability (percentage of saturation for a given land use type) over grid 2 for a) original simulations and time 0 of new simulations, and b) 24 hr simulation valid at 00 UTC 9 September for Runb simulation.**

## 6. Statistical methodology and output files

The statistical verification results were generated with ENVIRON’s METSTAT software. The statistics were computed using observations every 3 hours. The statistical quantities we will focus on are:

- *mean absolute error (MAE)*- average of the absolute values of the differences between the model value and the observation value. Good indicator of accuracy. Similar to Root Mean Square Error, but does not overly weigh outlying points.

$$MAE = \frac{1}{N} \sum_{i=1}^N |\Phi_O - \Phi_P|$$

- *mean relative(bias) error(MRE)* - average of the differences between the model value and the observation value. Good indicator of bias.

$$MRE = \frac{1}{N} \sum_{i=1}^N (\Phi_O - \Phi_P)$$

All observations within the grid 3 or grid 4 region (as appropriate to the domain being verified) were used for the statistics generation, except for those that were flagged by the quality control procedure. However, even with the quality control procedure there were still several questionable values that were allowed to remain. The majority of these were from the COAST observations.

As was done for previous projects, the final MM5 runs were set to output the simulation results every hour. A complete set of fields were output for all model grids, including u, v, w wind components, temperature, pressure, cloud variables, and precipitation. Eddy diffusion coefficients (or turbulent kinetic energy, TKE) were output in the previous project as the Gayno-Seaman TKE-based PBL scheme was used then. The final simulations in the current project used the MRF PBL which does not compute TKE and thus that field is not output. These were converted to CAMx-ready fields with software developed by ENVIRON.

## **7. Sensitivity Simulations**

### **7.1. Introduction**

The sensitivity simulations focused on the 24-hour period of 0000 UTC 8 September 1993 to 0000 UTC 9 September 1993. More than 20 different simulations were performed in the process of investigating the sensitivity of the MM5 results to various parameterizations, options, and grid resolution. The series of experiments can be generally categorized as control simulations, PBL tests, microphysics tests, and FDDA tests.

We will first present the basic descriptive results of the numerous sensitivity tests, as they relate to the main issues of MM5 performance that we were investigating, namely the weak sea breeze development, low daytime wind speed bias, and creation of large convective cells. After the descriptive results, we include a Discussion section which will attempt to tie the evidence together to explain the reasons for the behavior. Table 3 gives an overall summary of the individual runs. The "Run tag" descriptors will be used in the following sections to refer to specific simulations.

**Table 3 : MM5 sensitivity runs.**

Run Tag	No. grids	Duration	Micro-physics	Cu parm	PBL	Bucket scheme	Shallow cu	Iz0topt	Imvdif	FDDA grid ndgng
Runorig4	4	9/8/00-9/12/06	Schultz	Grell	G-S MY	NO	NO	NA	NA	YES BL, UA
Runold2	2	9/8/00-9/9/00	Schultz	Grell	G-S MY	NO	NO	NA	NA	NO
Runa	2	9/8/00-9/9/00	Simple ice	KF2	MRF	YES	NO	0	1	NO
Runa4	4	9/8/00-9/9/00	Simple ice	KF2	MRF	YES	NO	0	1	NO
Runb	2	9/8/00-9/9/00	Reis1	KF2	MRF	YES	NO	0	1	NO
Runc	2	9/8/00-9/9/00	Reis 1	KF2	G-S MY	YES	NO	NA	NA	NO
Rund	2	9/8/00-9/9/00	Reis1	KF2	ETA MY	YES	NO	NA	NA	NO
Runold4	4	9/8/00-9/9/00	Schultz	Grell	G-S MY	NO	NO	NA	NA	NO
Rune	3	9/8/00-9/9/00	Reis1	KF2	ETA MY	YES	NO	NA	NA	NO
Runf	3	9/8/00-9/9/00	Reis1	KF2	MRF	YES	YES	0	1	NO
Runf2	3	9/8/00-9/9/00	Reis1	KF2	MRF	YES	NO	0	1	NO
Rung	3	9/8/00-9/9/00	Reis1	KF2	MRF	YES	YES	2	0	NO
Runh	3	9/8/00-9/9/00	Reis1	KF2	MRF	YES	YES	2	1	NO
Runi	3	9/8/00-9/9/00	Reis1	KF2	ETA MY	YES	YES	NA	NA	NO
Runj	3	9/8/00-9/9/00	Reis 1	KF2	G-S MY	YES	NO	NA	NA	NO
Runj2	3	9/8/00-9/9/00	Reis 1	KF2	G-S MY modified	YES	NO	NA	NA	NO
Runk	3	9/8/00-9/9/00	Reis 1	KF2	Blackadar	YES	NO	NA	NA	NO
Runl	3	9/8/00-9/9/00	Simple ice	KF2	MRF	YES	NO	0	1	NO
Runm	3	9/8/00-9/9/00	Reis 2	KF2	MRF	YES	NO	0	1	NO
Runn	3	9/8/00-9/9/00	Schultz	KF2	MRF	YES	NO	0	1	NO
Runo	3	9/8/00-9/9/00	Reis 1	KF2	G-S MY	YES	NO	NA	NA	YES BL, UA
Runnew4	4	9/8/00-9/12/06	Reis 1	KF2	MRF	YES	NO	0	1	YES UA ONLY
Runnew3	3	9/8/00-9/12/06	Reis 1	KF2	MRF	YES	NO	0	1	YES UA ONLY
Runnew4b	4	9/8/00-9/12/06	Reis 1	KF2	MRF	YES	NO	0	1	YES UA>.85

## 7.2. Control Simulations

Runorig4 refers to the previous project's 4-grid simulation. A 24hr control simulation (Runold4) was produced using the same model options as the original 4-grid run (Runorig4), with a few important differences. Runorig4 was a 6-day simulation, initialized at 00 UTC 6 September while Runold4 was initialized at 0000 UTC 8 September. Also, the Runorig4 simulation used analysis nudging throughout its entire integration while the Runold4 simulation has no analysis (or observation) nudging at all. The purpose of the simulation was to determine whether the same general characteristics (and problems) in the simulation occurred with the new version, and improved SST and terrain. Figure 4 and Figure 5 show the 6 hr precipitation and surface wind fields over grid 3 for both simulations, valid at 1800 UTC 8 September (18 hrs into the simulation). The Runold4 simulation appears to be "worse" than the Runorig4 simulation in terms of spotty precipitation and outflow boundaries, but the differences are explainable by the strong diffusive and upscale-concentrating effect of the analysis nudging in the Runorig4 simulation. This diffusive effect will be shown more clearly in a simple experiment described in Section 7.5 and the upscale-concentration effect is discussed in Section 7.6. The abundance of spotty precipitation and outflow boundaries in the Runold4 simulation are consistent with the same features noted in the previous project. It can also be noted in Figure 4b that smaller-scale cells identify where grid 4 is located. The radar summary charts for 8-9 September (not shown) do show isolated convection but not anywhere near the frequency or small scale that is occurring in the Runold4 simulation. The outflow boundaries appear to swamp much of the sea breeze feature development. The tests in the following sections were conducted in order to better understand and solve these problems.

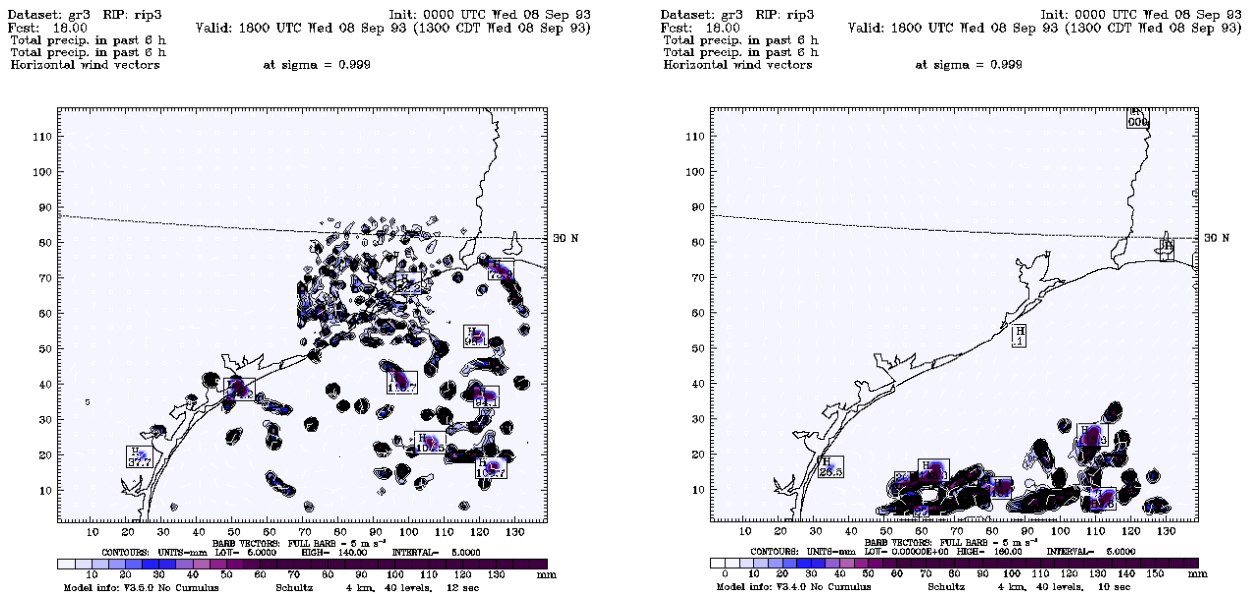


Figure 4 : 6 hr precipitation over grid 3 valid at 1800 UTC 8 September for a) Runorig4, and b) Runold4.

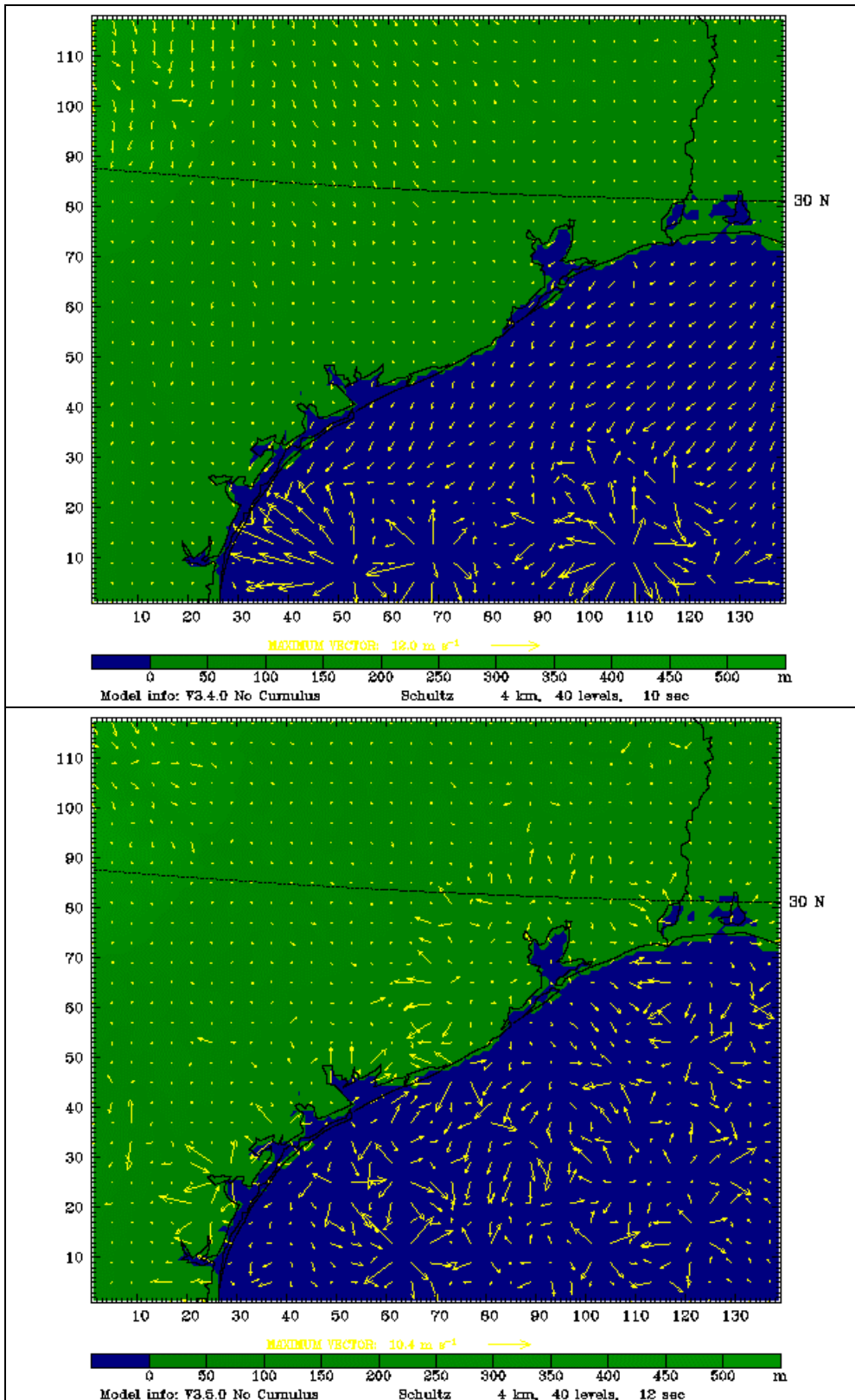


Figure 5 : Surface winds over grid 3 valid at 1800 UTC 8 September for a) Runorig4, and b) Runold4.

### **7.3. PBL Tests**

A series of tests were run to investigate the effect of the PBL parameterization on the simulation. Tests were first run on 2 grids because they are more computationally efficient. Tests were done to compare the different PBL schemes as well as to test some simple modifications and options within some of the schemes.

#### **7.3.1. Two-grid PBL tests**

A series of tests was first done with 2-grid simulations to compare the effects of the different available PBL parameterizations. Runb, Runc, and Rund are all 2-grid tests with the same microphysics (Reisner-1), the same cumulus parameterization (KF2 on both grids), the soil temperature model, and the bucket soil moisture model. Runb uses the MRF PBL, Runc uses the Gayno-Seaman (GS) Mellor-Yamada (MY) PBL, and Rund uses the ETA MY PBL. An additional 2-grid test was performed with the same options as Runb (MRF PBL) except using the simple ice microphysics instead of the Reisner 1 microphysics.

The 6 hr precipitation fields valid at 1800 UTC 8 September for the 4 simulations are shown in Figure 6. The GS PBL appears to have the least occurrence of the spotty precipitation on this scale, although the fields in all 4 simulations look better than in the Runold4 simulation (Figure 4b). The surface wind fields at the same time (Figure 7) do not show as many outflow boundaries as in the Runold4 simulation either. The ground temperature fields shown in Figure 8 show the highest temperatures with the GS PBL and the lowest with the MRF PBL runs, with the ETA MY PBL in the middle. Generally, the ground temperature with the MRF PBL tended to have the least amplitude in its diurnal variation while the ground temperature in the GS PBL simulation had the greatest amplitude.

The statistics plots in Figure 9-Figure 11 show bias and MAE, error for temperature, wind speed and specific humidity, for the 4 simulations described above as well as for the Runold2 simulation (closest to the previous original run's options). The temperature statistics plots in Figure 9 show that simulation with the ETA MY PBL has the least temperature error during the night and early evening (by about 1C) although its error during the day is similar to the simulations using the MRF PBL. The GS PBL simulations have the worst temperature error during the day (up to 1C worse) because of a stronger warm bias. The wind speed statistics show that the run with the ETA MY PBL has the least negative bias and the least error of all 5 simulations, and the GS PBL has the greatest error during the day. The specific humidity statistics (Figure 11) show that the runs with the MRF scheme have a dry bias during the day and that the run with the Ea PBL has the greatest error during the night and early morning.

Based on these runs, the ETA PBL appears to perform the best in terms of temperature and wind speed statistics. The GS PBL appears to have the least amount of spotty precipitation on this scale though. The next series of experiments were done with 3 grids (36 km, 12 km, and 4 km grid spacings) in order to better determine which scheme performed the best on smaller scales. One strong caveat in the grid 2 results is that the cumulus parameterization is active on both grids and may thus be providing additional mixing and the release of convective instability. The cumulus parameterization should

not be used on the grid 3 scale though and thus the results including that grid could be markedly different.

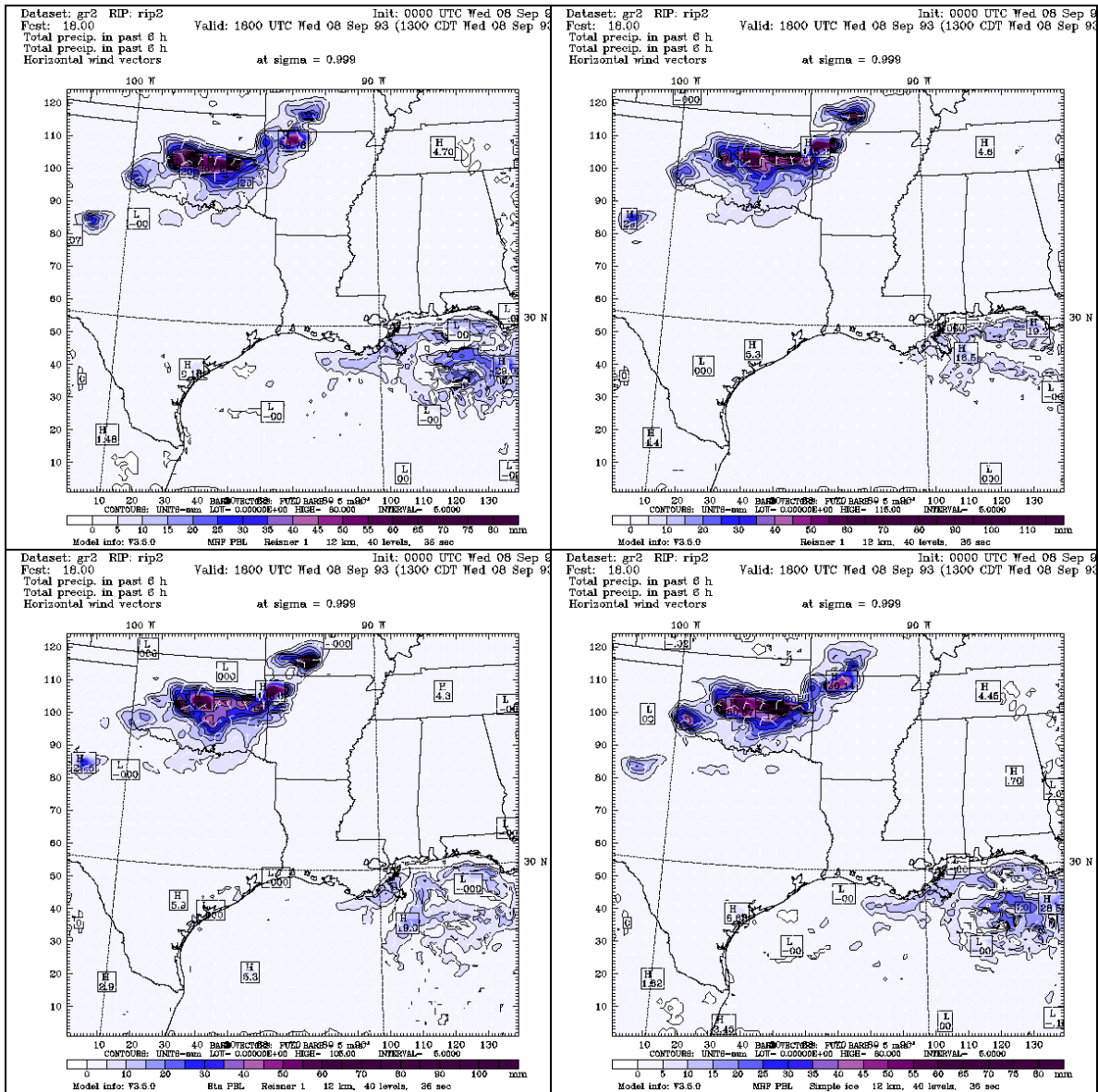


Figure 6 : 6-hr precipitation valid over domain 2 at 1800 UTC 8 September for a) Runb (MRF PBL), b) Runc (GS PBL), c) Rund (ETA MY PBL), and d) Runa (MRF PBL and simple ice microphysics).

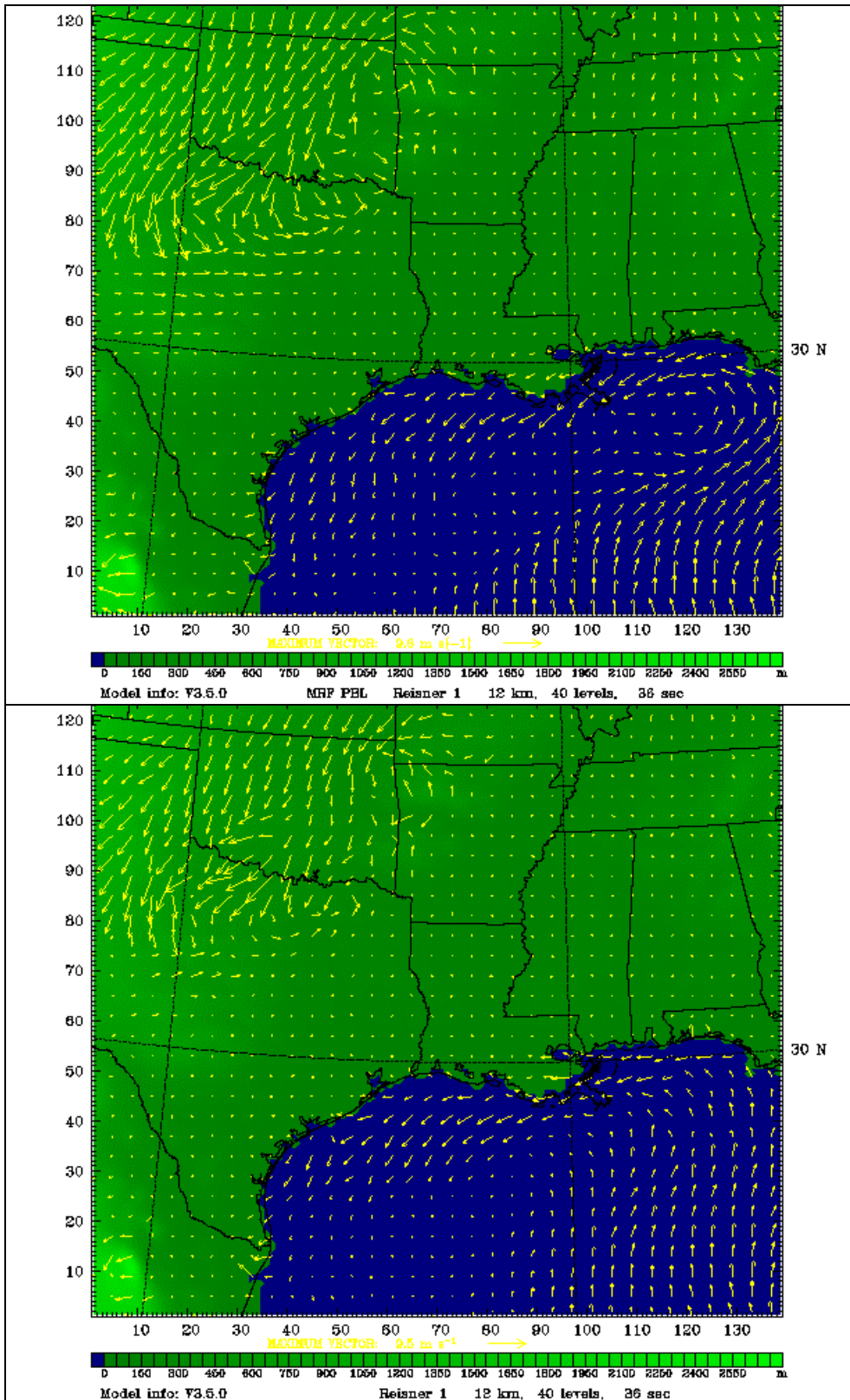


Figure 7. Surface winds valid over domain 2 at 1800 UTC 8 September for a) Runb (MRF PBL), b) Runc (GS PBL), c) Rund (ETA MY PBL), and d) Runa (MRF PBL and simple ice microphysics).

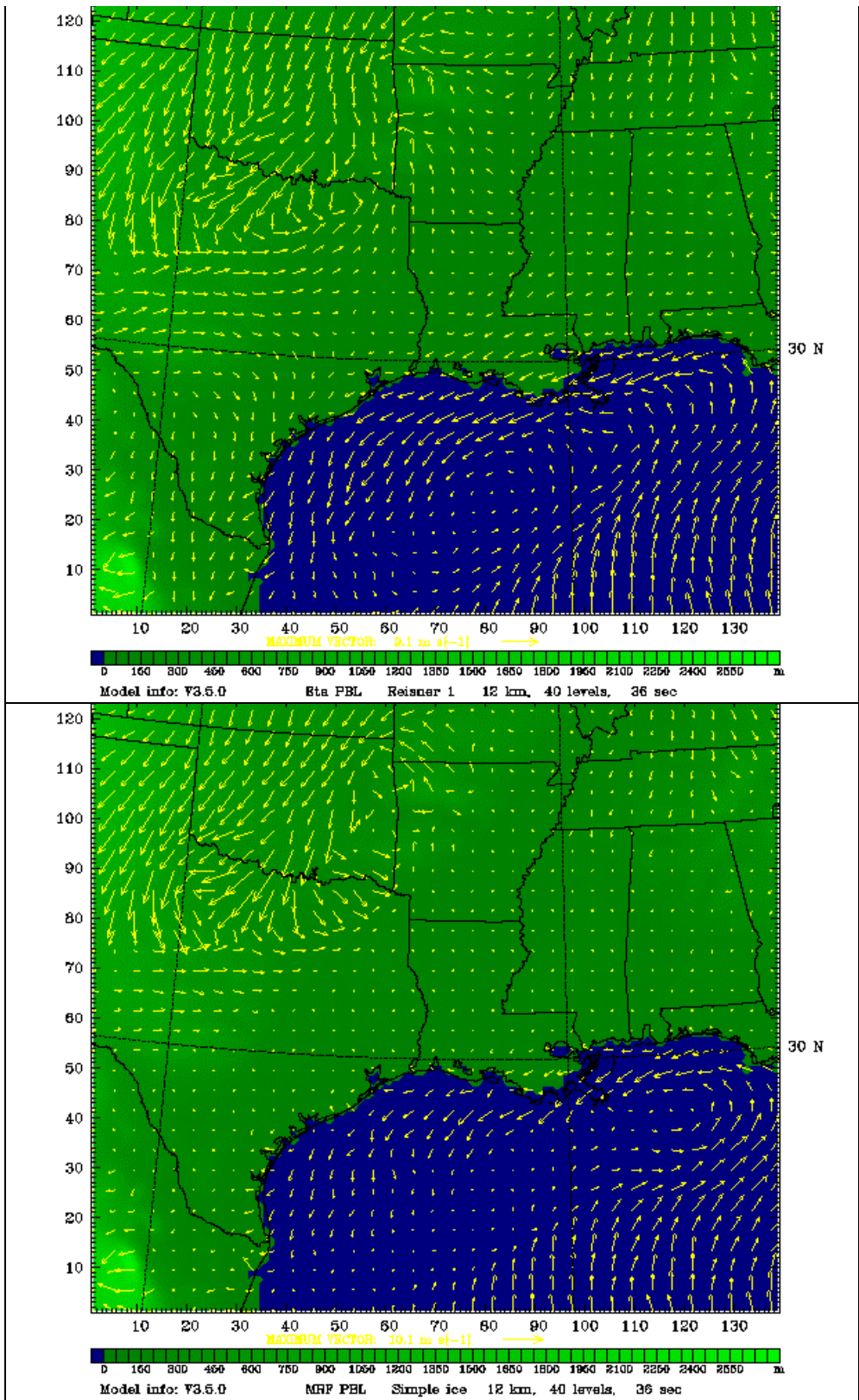


Figure 7 : Concluded.

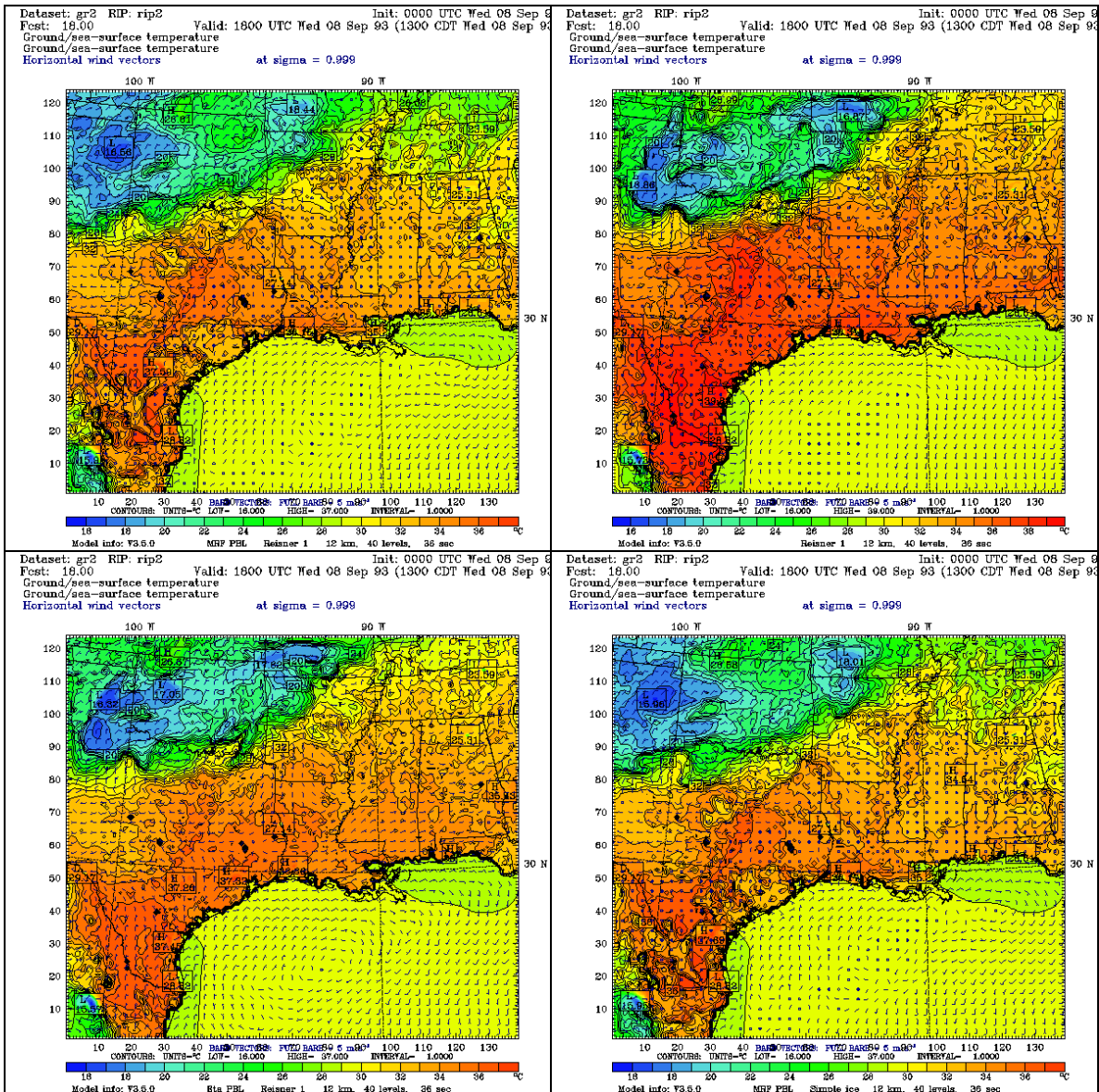
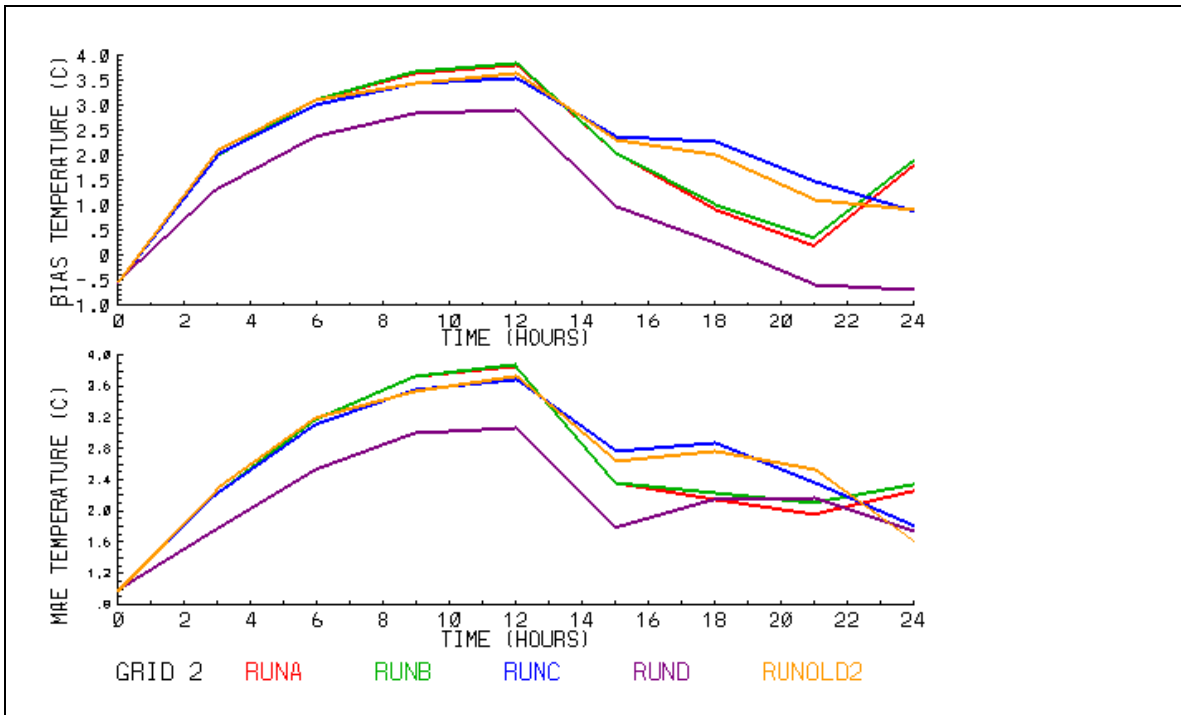
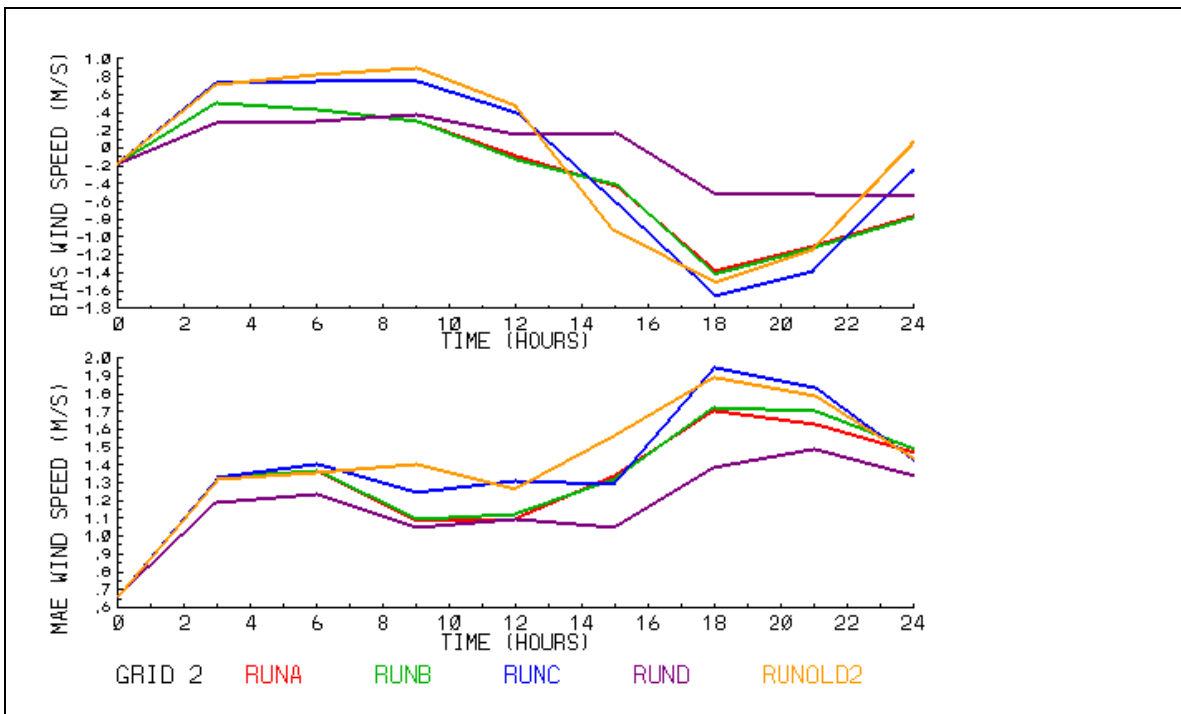


Figure 8 : Ground temperature valid over domain 2 at 1800 UTC 8 September for a) Runb, b) Runc, c) Rund, and d) Runa.



**Figure 9 : Temperature statistics from 0000 UTC 8 September through 0000 UTC 9 September over domain 2 for Runa (MRF PBL and simple ice, red line), Runb (MRF PBL, green line), Runc (GS PBL, blue line), Rund (ETA MY PBL, purple line), and Runold2 (GS PBL, Schultz microphysics, Grell cu param, orange line). Top graph is bias plot, bottom is MAE plot.**



**Figure 10 : Wind speed statistics from 0000 UTC 8 September through 0000 UTC 9 September over domain 2 for Runa (MRF PBL and simple ice, red line), Runb (MRF PBL, green line), Runc (GS PBL, blue line), Rund (ETA MY PBL, purple line), and Runold2 (GS PBL, Schultz microphysics, Grell cu param, orange line). Top graph is bias plot, bottom is MAE plot.**

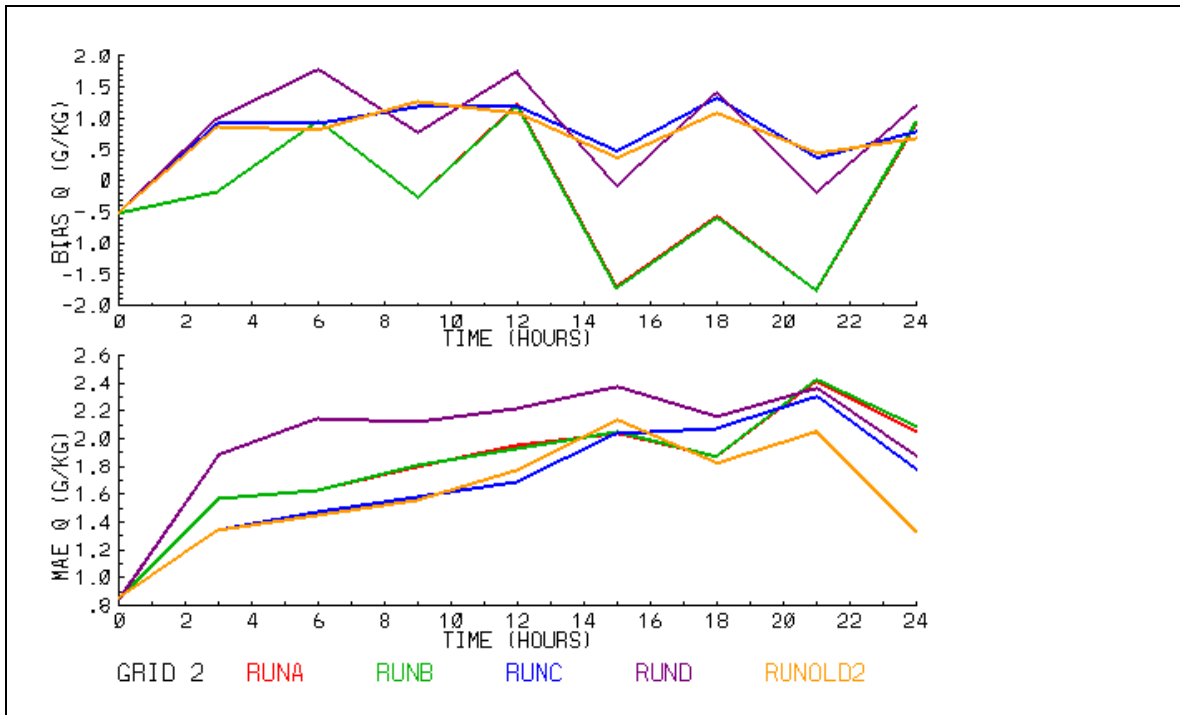


**Figure 11 : Specific humidity statistics over the time range 0000 UTC 8 September through 0000 UTC 9 September over domain 2 for Runa (MRF PBL and simple ice, red line), Runb (MRF PBL, green line), Runc (GS PBL, blue line), Rund (ETA MY PBL, purple line), and Runold2 (GS PBL, Schultz microphysics, Grell cu param, orange line). Top graph is bias plot, bottom is MAE plot.**

### 7.3.2. Three-grid PBL tests

The next set of tests was run on 3 grids with the various PBL schemes. A crucial difference between the 2- and 3- grid runs is that the spacing of the third grid precludes use of the cumulus parameterization scheme and thus forces any convection that would occur to the explicit scale. Runf2, Runj, Runk, and Rune all used the same options except for the PBL parameterization: MRF, GS, Blackadar, and ETA MY, respectively.

Figure 12 and Figure 13 show the 6 hr precipitation on grid 3 valid at 1800 UTC 8 September and 0000 UTC 9 September for all 4 simulations. The MRF PBL simulation shows the least amount of the spotty precipitation while the GS and ETA MY schemes show the greatest amount of spotty precipitation. It should be noted that these results are at odds with the 2-grid simulation results. All 4 simulations do appear to be developing a sea breeze circulation as shown by the surface wind plots in Figure 14, although the increased frequency of outflow boundaries in the GS and ETA MY simulations does overwhelm the sea breeze in places.

The PBL height plots in Figure 15 are especially interesting. These plots show the PBL height at 1800 UTC 8 September (near noon local time) for all 4 simulations. The PBL height in the GS and ETA MY simulations is in the 1000-1500m range over land while it is in the 2000-2500m range over land in the MRF PBL simulation and slightly less in the Blackadar PBL simulation. The small areas of lower PBL height within the plots are due to areas where cloud shading did not allow the ground surface to heat up as much. The

spots of higher PBL height within the GS PBL run are places where the TKE (which defines the PBL in the GS and ETA MY PBL schemes) has advected upward in "plumes" (clearly seen in vertical cross-sections, not shown here). The ETA MY scheme is also a TKE-based scheme but there is not advection of TKE included with the implementation of this scheme in the MM5 model; consequently, the ETA MY PBL heights do not show the same plumes. The implementation of the MM5 GS MY PBL does include an option to turn off the advection - the default of including advection was used in all simulations here. We do not have the PBL height verification information available for this time period. Based on past experience though, we feel that the PBL heights in the GS and ETA MY PBL schemes are too low for the strong heating situation on this day, and the MRF PBL heights are likely more realistic, although perhaps on the high side. The RAMS simulations over the same time period had PBL heights in the 2000m range.

The statistics for these runs on grid 3 for temperature, wind speed, and specific humidity are shown in Figure 16-Figure 18. The temperature statistics show the ETA MY PBL with the least error at night but the greatest error during the day. The wind speed statistics also show the ETA MY PBL with the least error throughout much of the day although its errors are comparable to the MRF scheme late in the day (2100-0000 UTC period).

Statistically, these tests show that the ETA MY PBL scheme may have the least error, although the plots show that other factors also need to be considered. The PBL heights in the GS and ETA MY PBL schemes seem to be too low, and both these schemes over-produce spotty grid-scale convection on grid 3. The convective cells then grow to produce outflow boundaries and tend to overwhelm the development of the sea breeze.

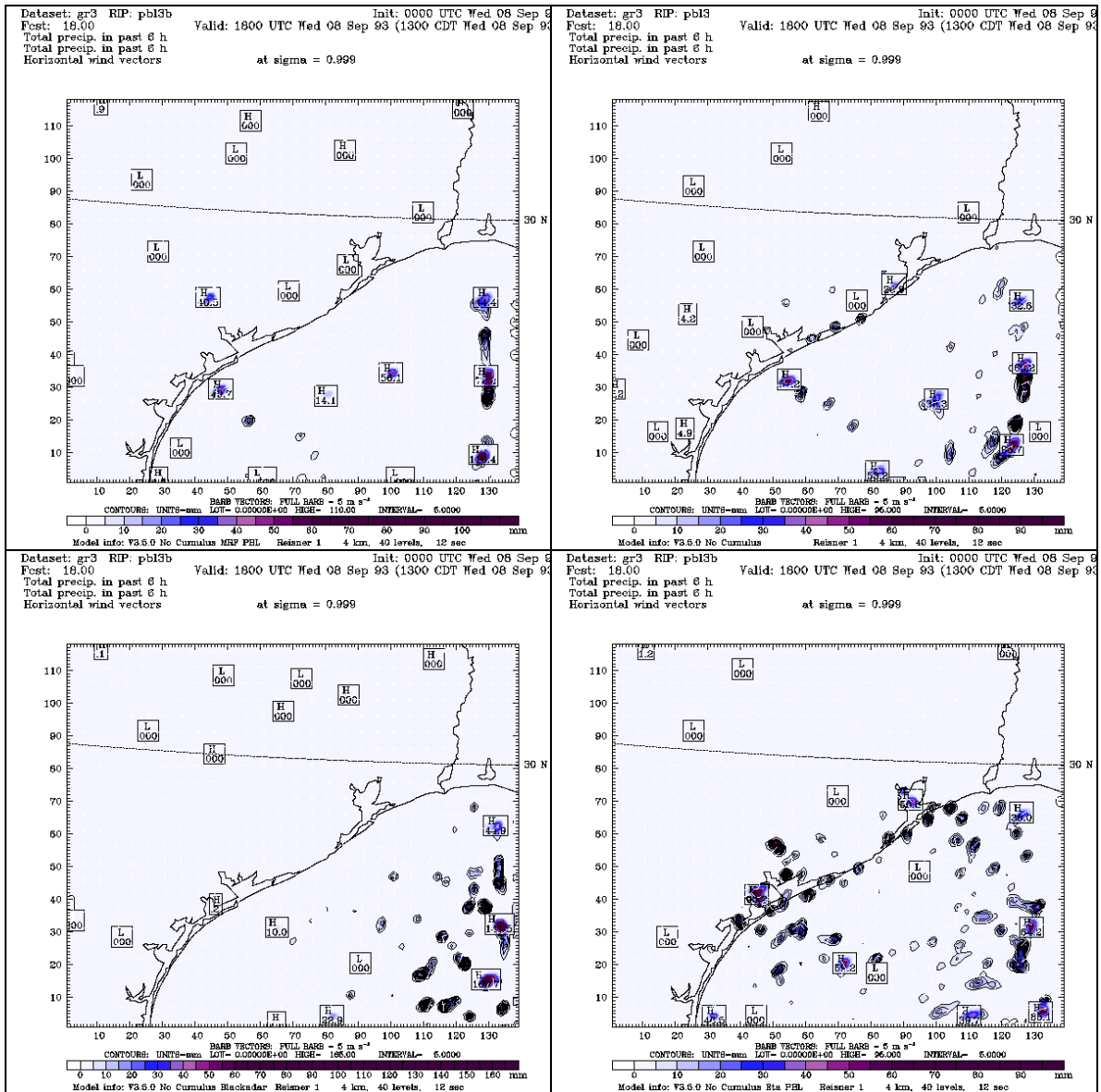


**Figure 12 : 6-hr precipitation on grid 3 at 1800 UTC 8 September for a) Run2 (MRF pbl), b) Runj (GS pbl), c) Runk (Blackadar pbl), and d) Rune (ETA MY pbl).**



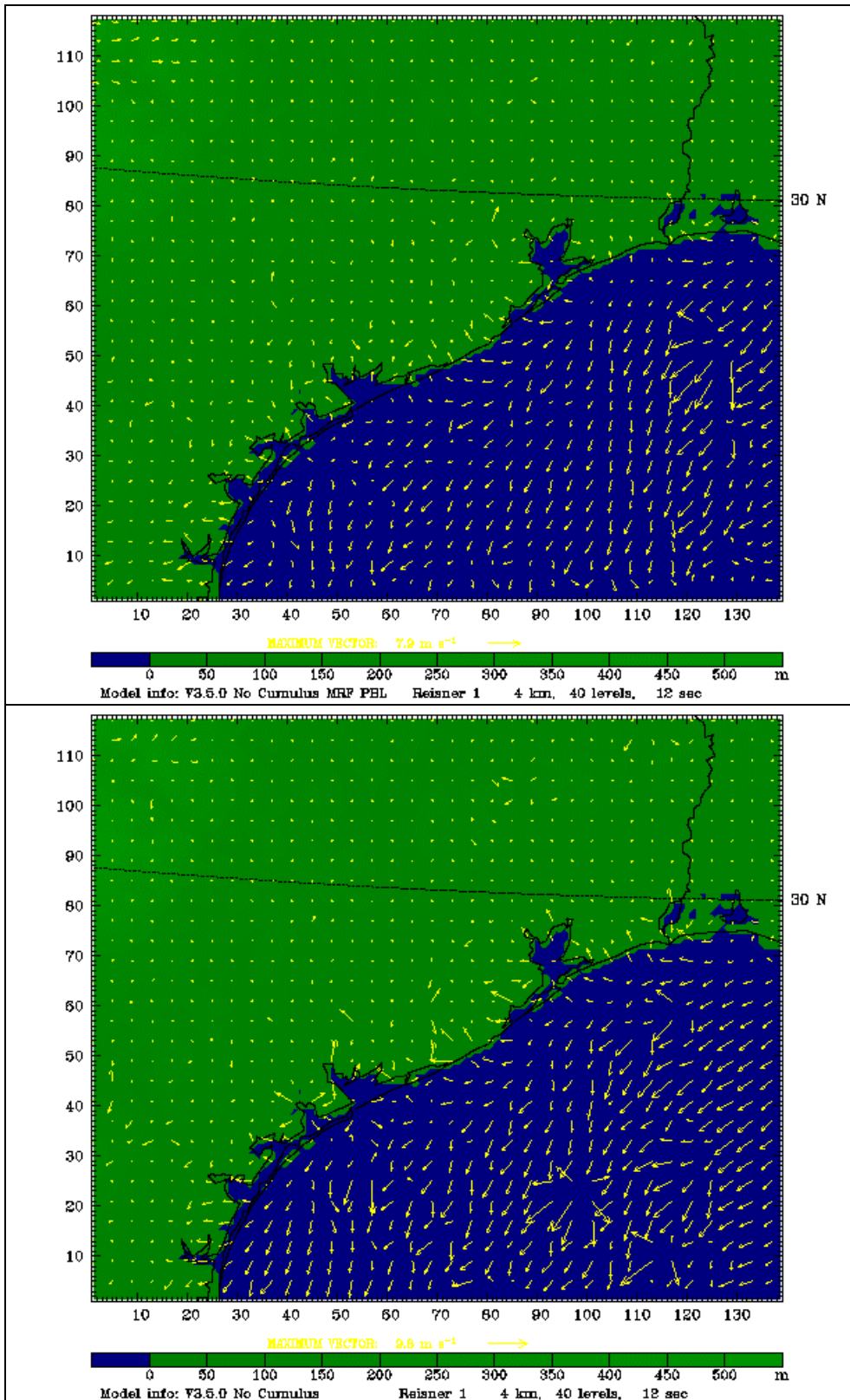


Figure 14 : Surface winds on grid 3 at 1800 UTC 8 September for a) Runf2 (MRF pbl), b) Runj (GS pbl), c) Runk (Blackadar pbl), and d) Rune (ETA MY pbl).

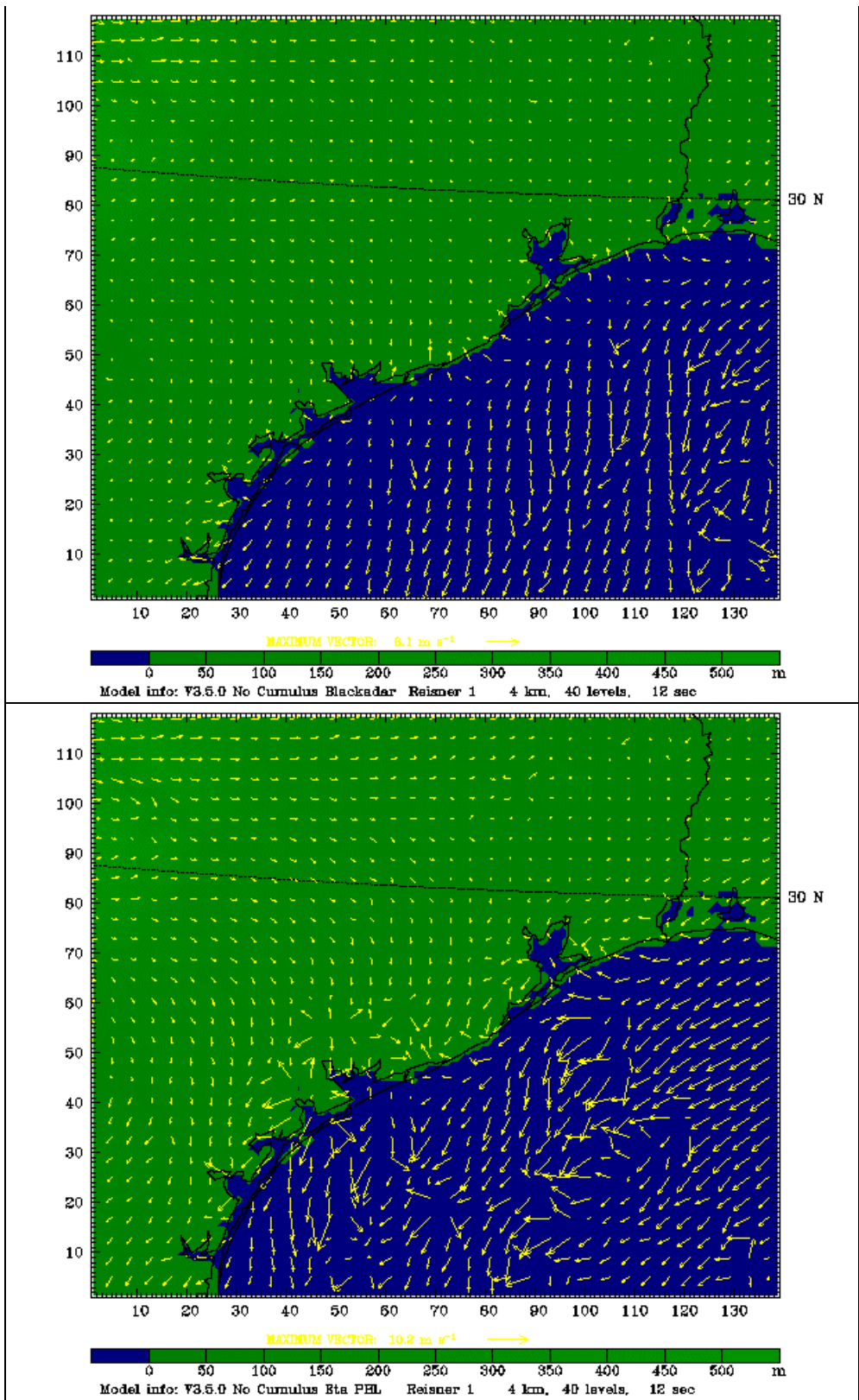


Figure 14 : Concluded.

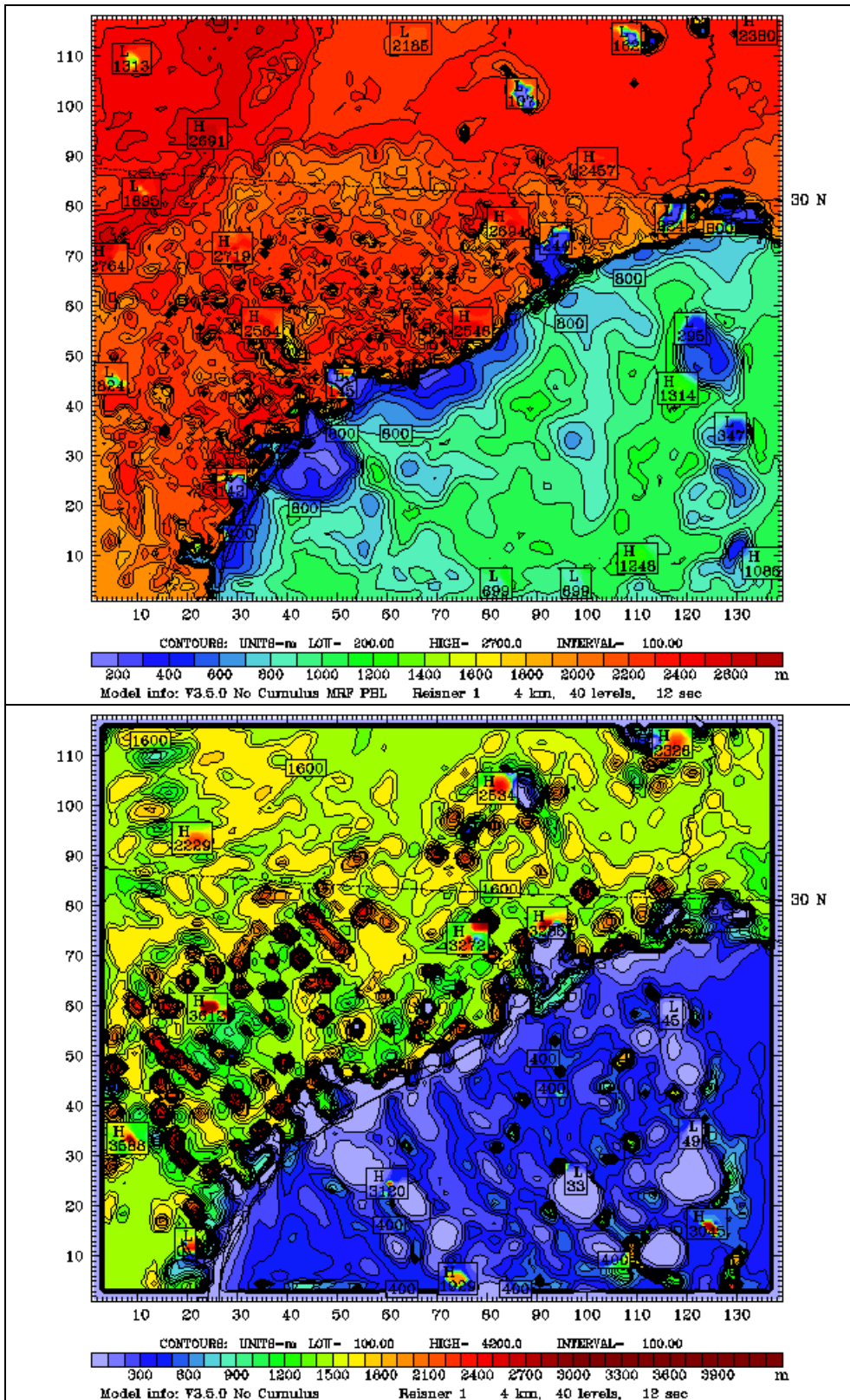


Figure 15 : PBL height (m) on grid 3 at 1800 UTC 8 September for a) Runf2 (MRF pbl), b) Runj (GS pbl), c) Runk (Blackadar pbl), and d) Rune (ETA MY pbl).

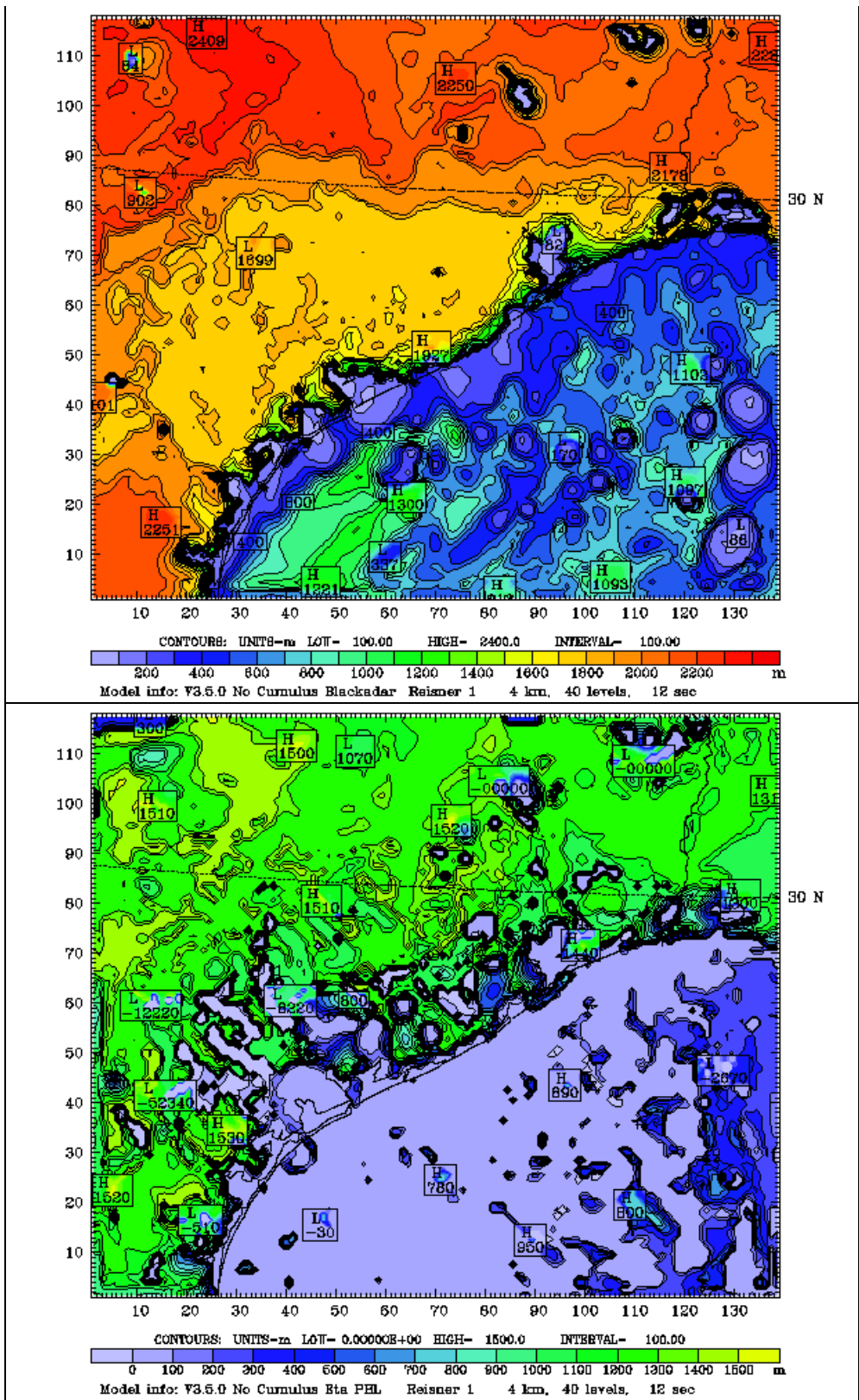
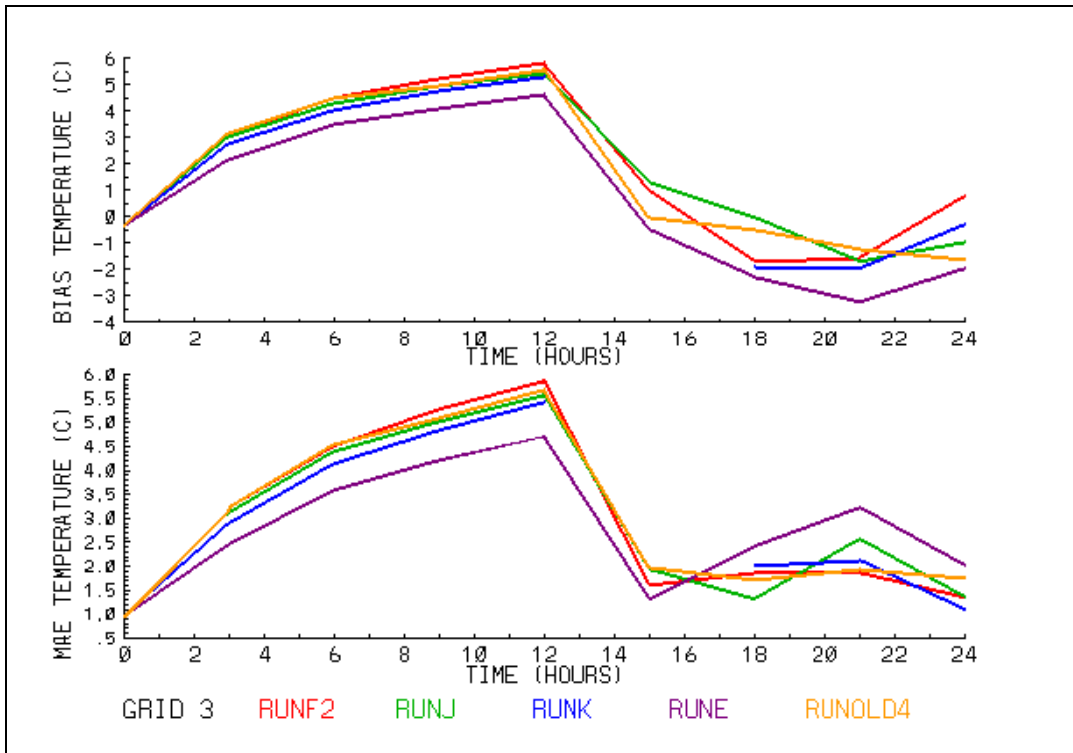
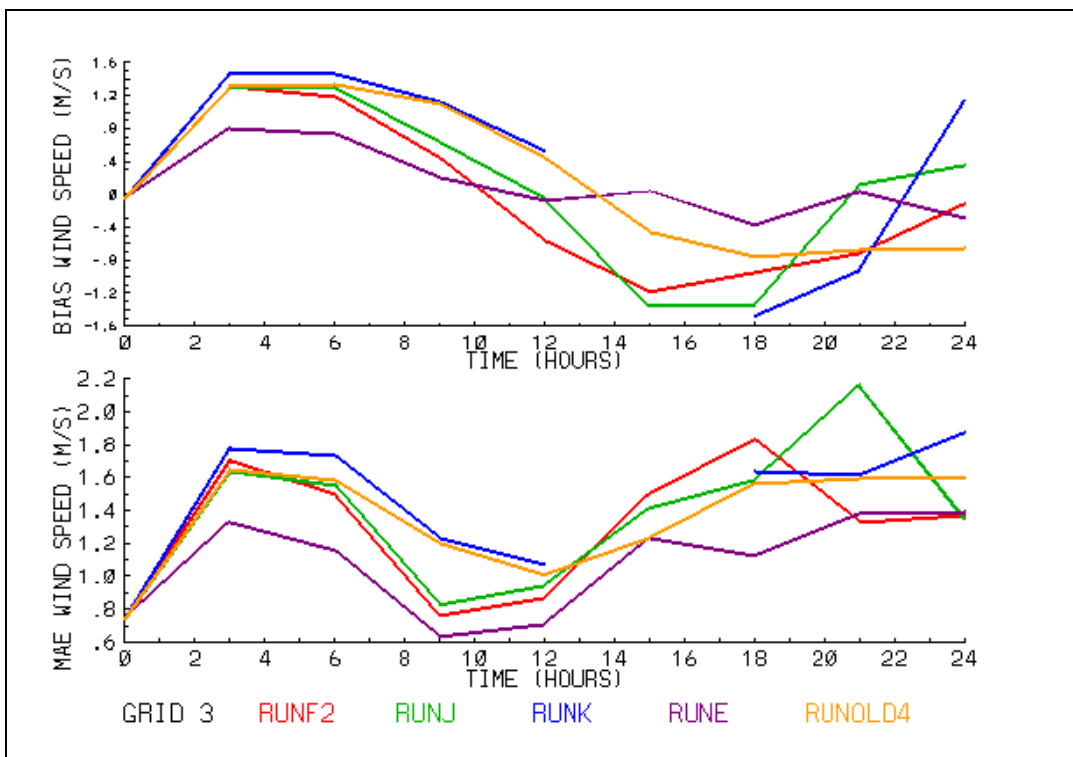


Figure 15: Concluded.



**Figure 16 : Temperature statistics for domain 3 for the Runf2 (MRF, red line), Runj (GS, green line), Runk (Blackadar, blue line), Rune (ETA MY, purple line), and Runold4 (GS, different other options too, orange line) simulations. Top graph is bias, bottom is MAE. The blue curve has a break at 15 hrs because of a bad output file.**



**Figure 17: Wind speed statistics for domain 3 for the Runf2 (MRF, red line), Runj (GS, green line), Runk (Blackadar, blue line), Rune (ETA MY, purple line), and Runold4 (GS, different other options too, orange line) simulations. Top graph is bias, bottom is MAE. The blue curve has a break at 15 hrs because of a bad output file.**

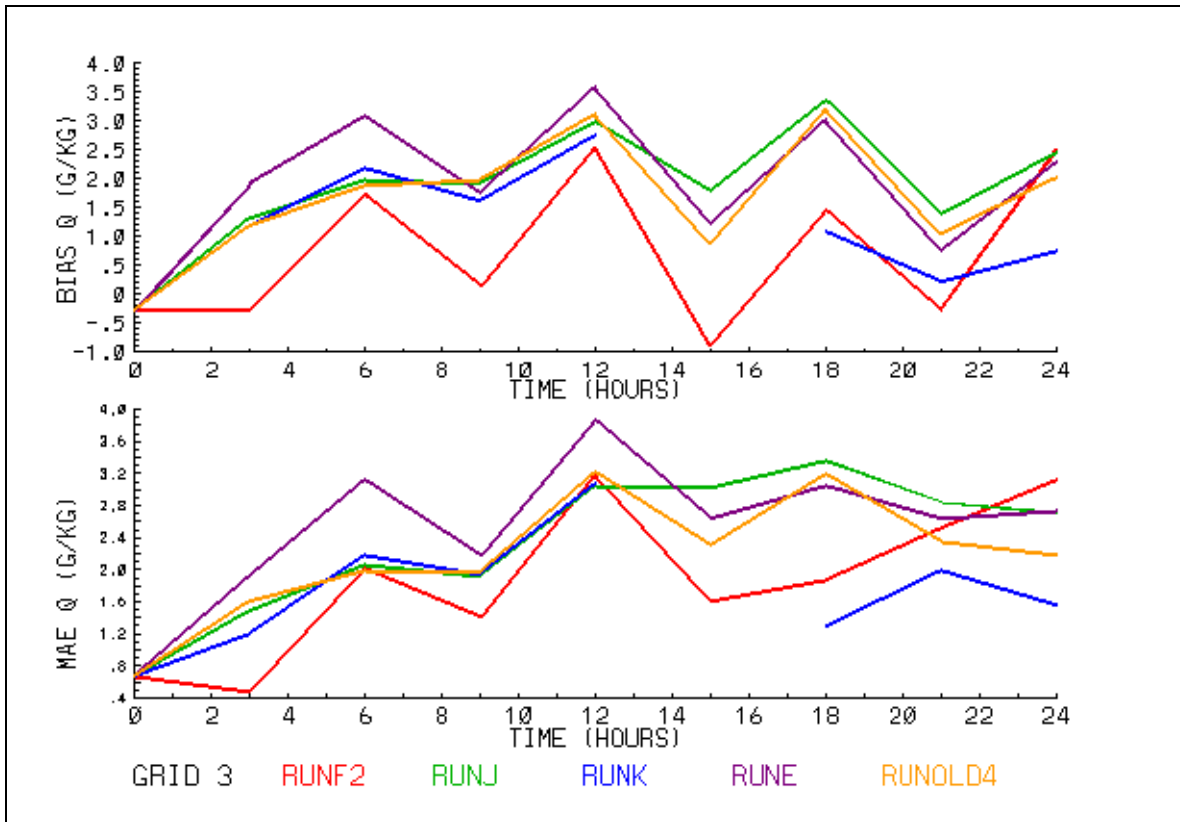


Figure 18 : Specific humidity statistics for domain 3 for the Runf2 (MRF, red line), Runj (GS, green line), Runk (Blackadar, blue line), Rune (ETA MY, purple line), and Runold4 (GS, different other options too, orange line) simulations. Top graph is bias, bottom is MAE. The blue curve has a break at 15 hrs because of a bad output file.

### 7.3.3. Shallow convection tests

A few tests were done with the shallow convection parameterization (ishallo=1) in the model. These tests were with the ETA MY (Runi and Rune, ishallo=1 in Runi) and MRF (Runf and Runf2, ishallo=1 in Runf) PBL schemes. When ishallo was turned on it was turned on for all 3 domains within the simulation. The results for Runi and Rune (both ETA MY PBL) were very similar as were the results for Runf and Runf2 (both MRF PBL); the greater difference was between the ETA MY and MRF PBL results.

### 7.3.4. MRF PBL tests

A few tests were also done with some of the options available within the MRF PBL scheme. These tests were with the Runh, Rung, Runf, and Runf2 simulations and involved turning the imvdif and iz0topt options on and off. See Table 1 for the specifics of each simulation. The imvdif option is for moist vertical mixing (vs. dry mixing) in clouds, and the iz0topt option controls how the thermal and moisture roughness lengths are calculated. Iz0topt=0 uses the Carlson-Boland method, and the same formulae are used over land and water. Iz0topt=2 uses the Zilitinkevich formulation and different formulae are used over land and water. Slightly better results were found with iz0topt=0 vs. iz0topt=2, and with imvdif=1 vs. imvdif=0, although the differences were minor. The temperature and wind speed statistics for these runs are shown in Figure 19 and Figure 20.

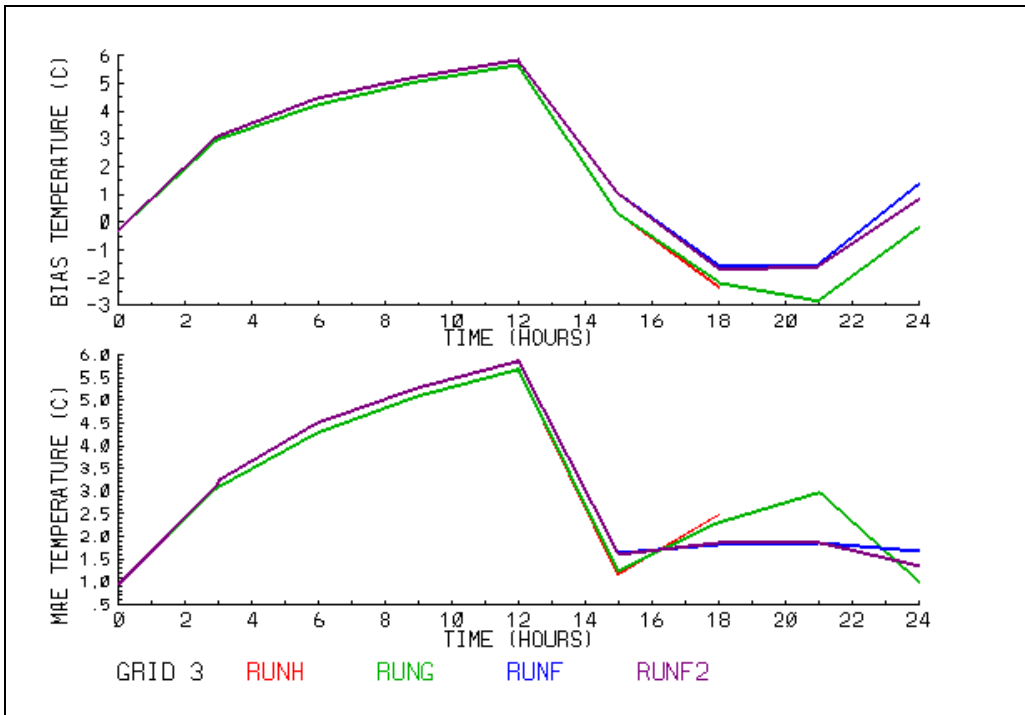


**Figure 19 : Temperature statistics for domain 3 for the Runh (red line), Rung (green line), Runf (blue line), and Runf2 (purple line) simulations. Top graph is bias, bottom is MAE. The A curve only runs to 18 hrs because the Runh simulation was killed at that point.**

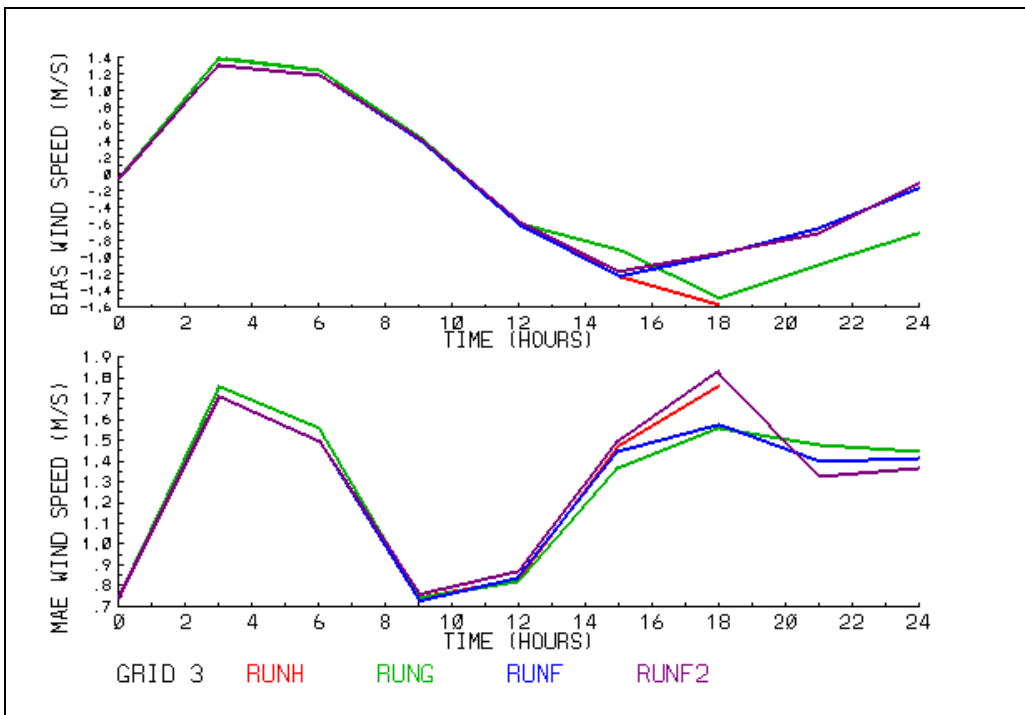


**Figure 20 : Wind speed statistics for domain 3 for the Runh (red line), Rung (green line), Runf (blue line), and Runf2 (purple line) simulations. Top graph is bias, bottom is MAE. The A curve only runs to 18 hrs because the Runh simulation was killed at that point.**

### **7.3.5. Gayno-Seaman PBL tests**

The previous tests indicated that the PBL height was probably too low in the daytime with the GS PBL (and also the ETA M-Y PBL scheme). The PBL height is especially important in terms of air quality simulations. The ground temperature associated with the GS PBL was higher than that of the other PBL parameterizations. We speculated that the GS PBL scheme was perhaps not mixing heat, moisture, and momentum upwards enough within the PBL and tried a simple modification to increase the vertical mixing. From looking at vertical cross-sections of potential temperature (not shown), we discovered that a significant super-adiabatic layer near the ground of several degrees was a consistent feature of the GS scheme. If the eddy diffusivity near the ground was too low, the low level temperatures would remain higher, and reduce the sensible heat flux from the ground.

We performed a simple modification to the GS scheme, where the K coefficients for heat diffusion as calculated were multiplied by a factor of 5. This experiment was the Runj2 simulation; the non-modified GS PBL run is the Runj simulation. One other difference is that grid 3 in the Runj2 simulation was started 12 hours into the Runj simulation and thus runs from the 12-24 hr point. This later initiation of grid 3 was done simply to save time; it is not expected that it would have a significant effect on the results.

The PBL heights at 1800 UTC 8 September for the 2 simulations are shown in Figure 21. As expected, the increased mixing results in an increase of the PBL height at 1800 UTC by about 500m, from 1000 to 1500m. The temperature, wind speed, and moisture statistics for these 2 runs are shown in Figure 22-Figure 24. Generally the modified GS PBL (increased mixing) performed better than the original scheme. In addition, the number and strength of the small-scale convective elements were reduced. The very simple modification seemed to improve the results.

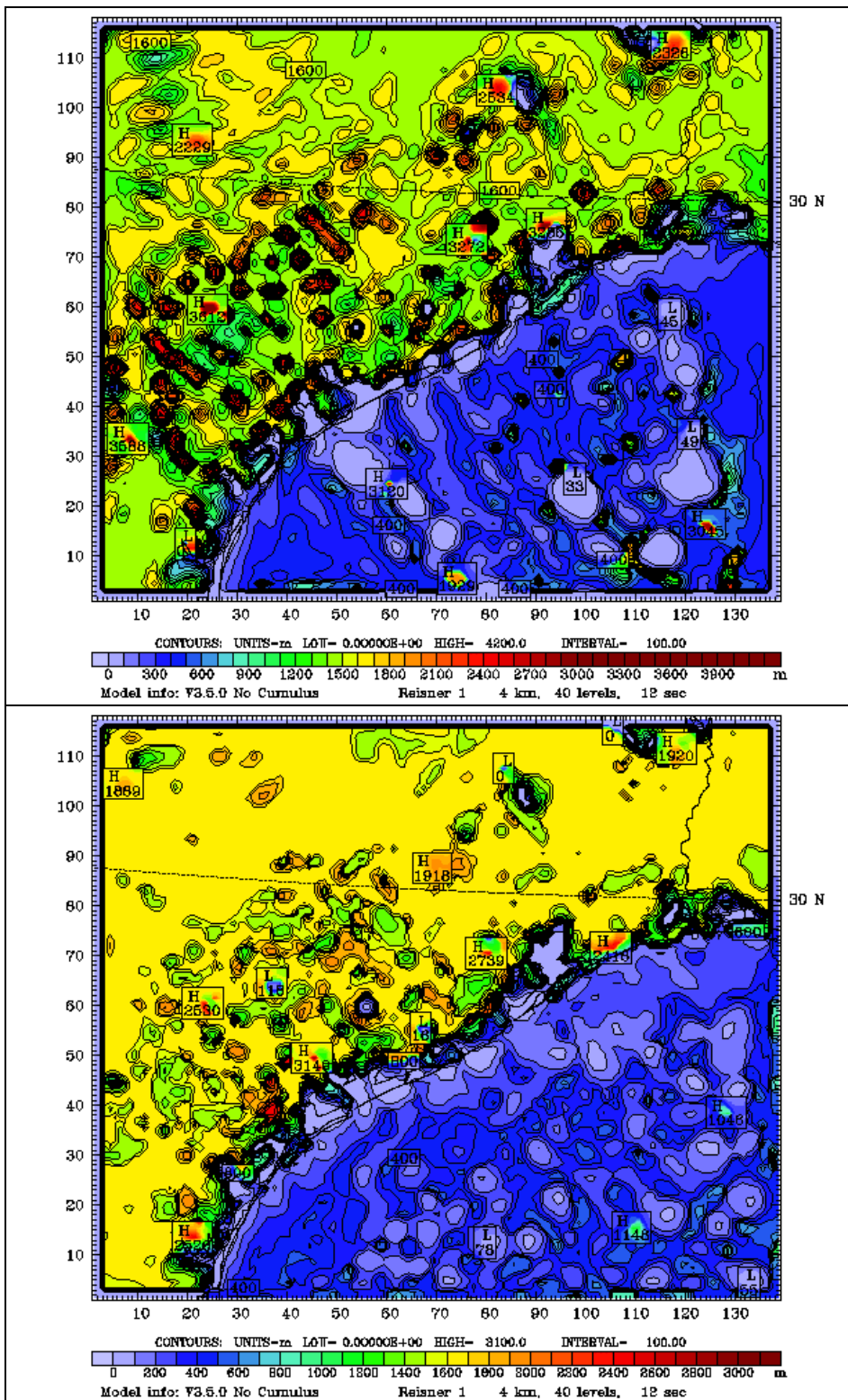
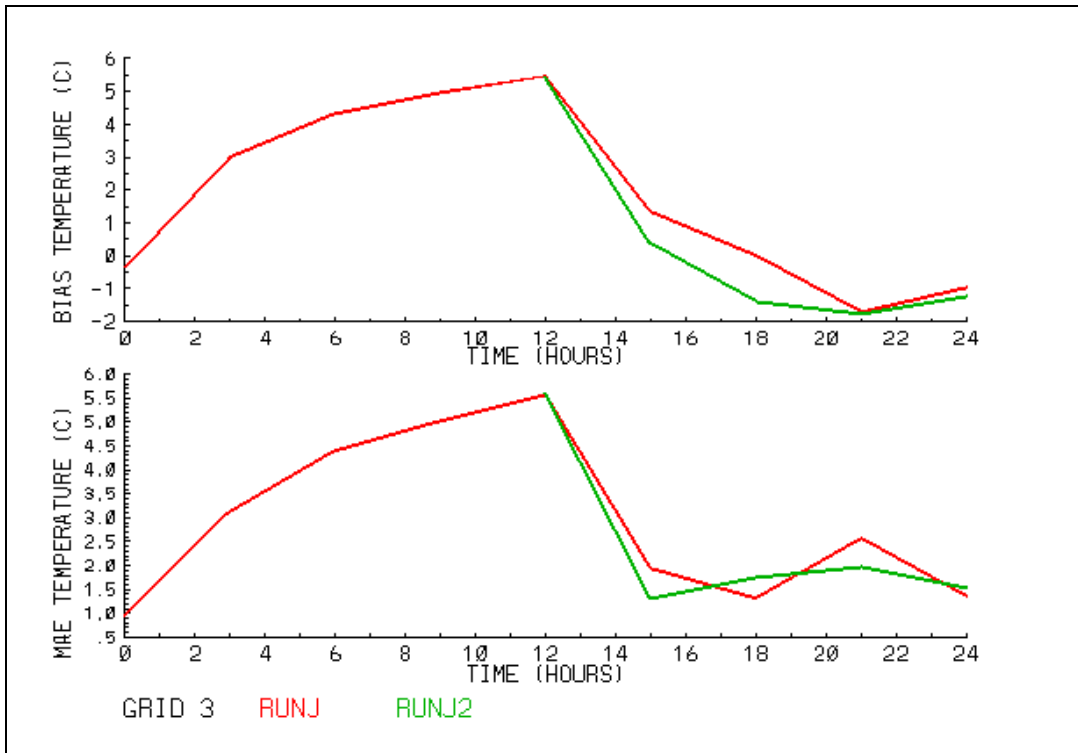
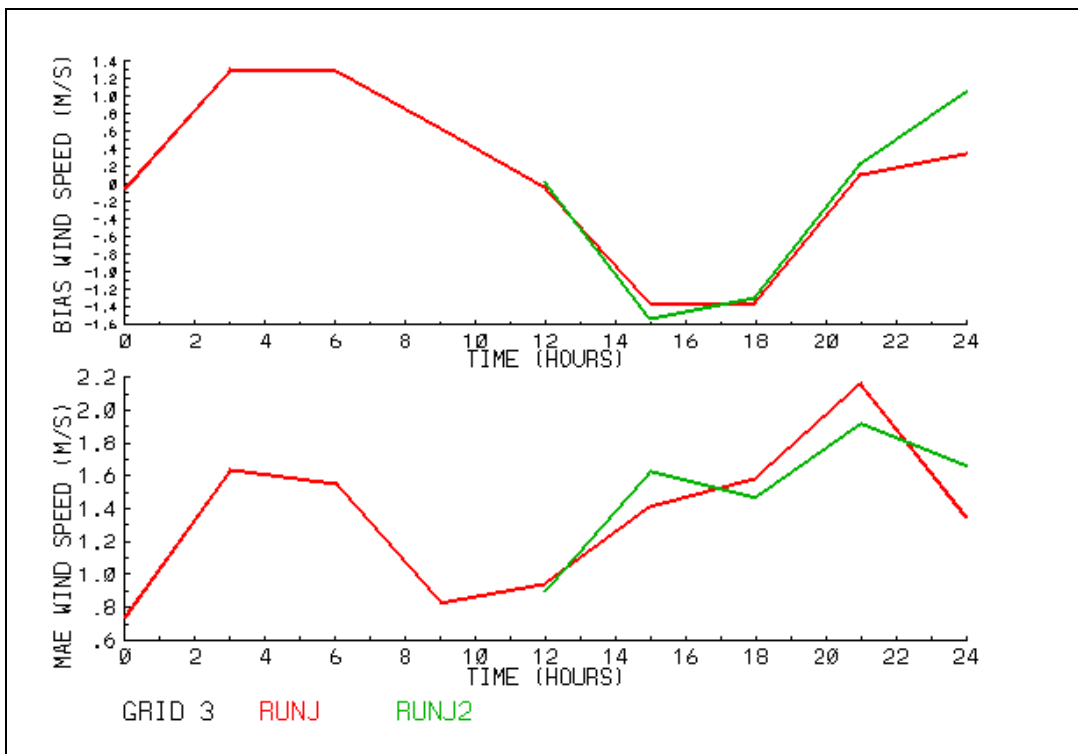


Figure 21 : PBL height at 1800 UTC 8 September for domain 3 for the a) Runj (original GS PBL scheme) and b) Runj2 (GS PBL scheme modified for increased mixing) simulations.



**Figure 22: Temperature statistics for domain 3 for the Runj (original GS PBL scheme, red line) and Runj2 (GS scheme modified for increased mixing, green line) simulations. Top graph is bias, bottom is MAE. The green curve runs from 12-24 hrs because the Runj2 simulation initialized grid 3 at 12 hrs.**



**Figure 23 : Wind speed statistics for domain 3 for the Runj (original GS PBL scheme, red line) and Runj2 (GS scheme modified for increased mixing, green line) simulations. Top graph is bias, bottom is MAE. The green curve runs from 12-24 hrs because the Runj2 simulation initialized grid 3 at 12 hrs.**

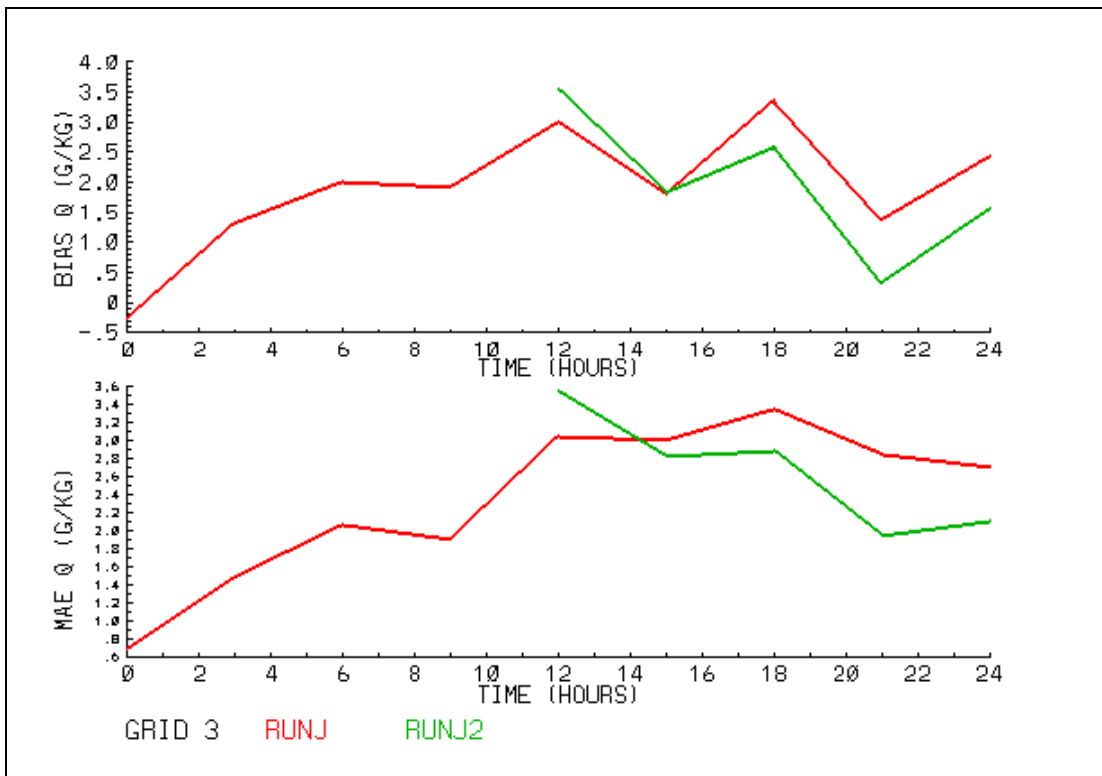


Figure 24 : Specific humidity statistics for domain 3 for the Runj (original GS PBL scheme, red line) and Runj2 (GS scheme modified for increased mixing, green line) simulations. Top graph is bias, bottom is MAE. The green curve runs from 12-24 hrs because the Runj2 simulation initialized grid 3 at 12 hrs.

#### 7.4. Microphysics tests

Tests were also completed to test the effect of the microphysical parameterization on the simulations. The Runf2, Runl, Runm, and Runn simulations all used the same parameterizations and options except for the microphysics scheme (Reisner-1, simple ice, Reisner-2, and Schultz, respectively). All 4 simulations had scattered precipitation throughout the domain. Statistically, there was virtually no difference in the temperature and wind speed statistics (shown in Figure 25) and only a very slight difference in the moisture statistics (shown in Figure 26). Based on these results and the PBL tests, we concluded that the microphysical parameterization was not the primary factor in the occurrence of the spotty convection in the simulations.

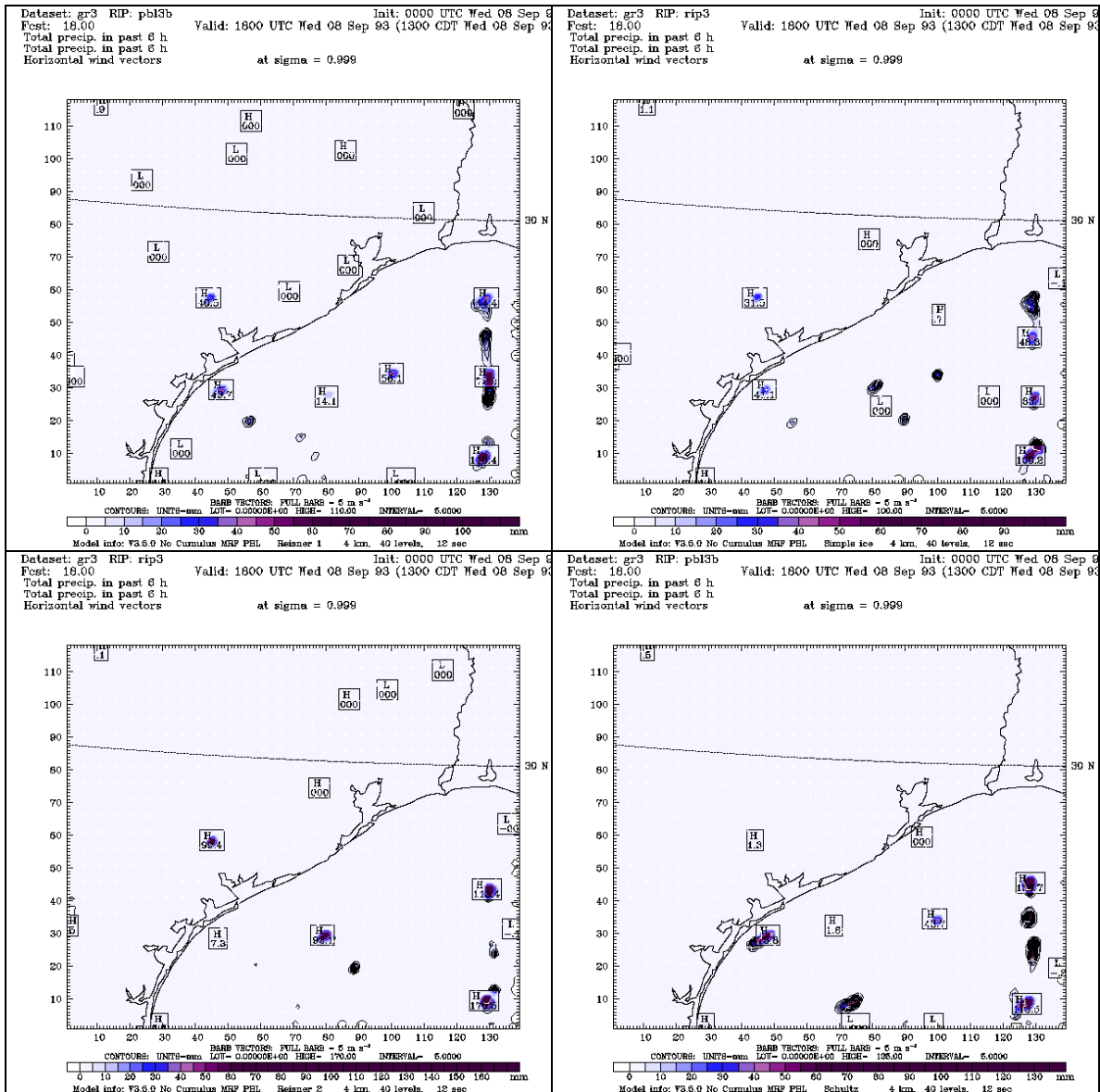


Figure 25 : 6-hr precipitation valid at 1800 UTC 8 September for a) Reisner-1, b) Simple ice, c) Reisner-2, and d) Schultz microphysics schemes.

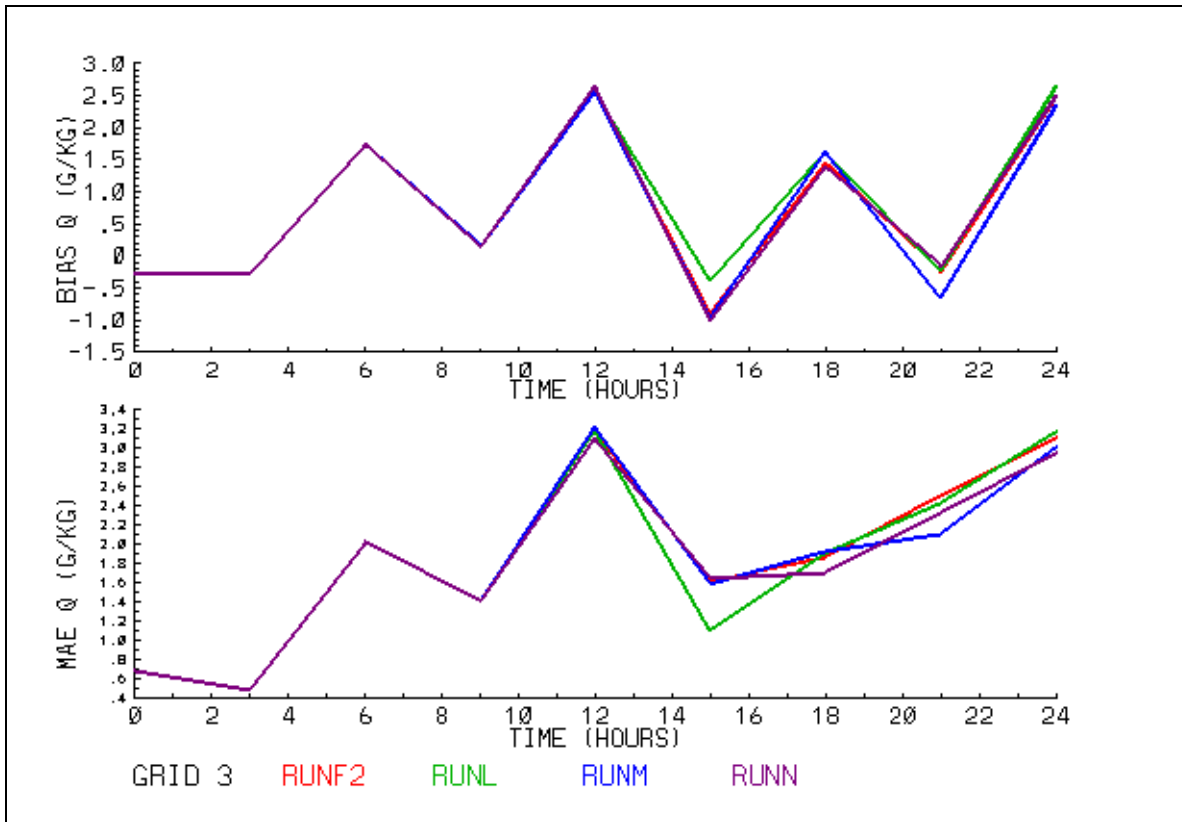


Figure 26: Specific humidity statistics for domain 3 for the Runf2 (Reisner-1, red line), Runl (Simple ice, green line), Runm (Reisner-2, blue line), and Runn (Schultz, purple line) simulations. Top graph is bias, bottom is MAE.

### 7.5. FDDA nudging effect test

One test was done to more cleanly compare the effects of nudging on the simulation. The Runo simulation used the same parameterizations and options as the Runj simulation (both used GS MY PBL, Reisner 1 microphysics, KF2 cumulus parameterization) except that grid nudging was also turned on in Runo. Both surface/boundary layer analysis nudging and upper air analysis nudging were used, for all 4 variables (T, q, u, and v) and on all 3 grids.

The 6-hr precipitation valid at 1800 and 0000 UTC for both simulations is shown in Figure 27. Although the diffusive effect of the nudging does not get rid of the spotty convection, it does seem to be organized on a larger scale in the grid nudging simulation (similar to the results seen in the Runorig4 simulation shown in Figure 4a). This upscale organization is discussed in more detail in Section 7.6.

The surface winds valid at 1800 UTC are shown in Figure 28. These 2 fields especially illustrate some of the problems associated with grid nudging. The winds in the Runo (grid nudging simulation) do not show the sea breeze development apparent in the Runj simulation (no nudging). The nudging acts to both diffuse the model fields and also by definition "nudges" the model fields towards a separate analysis. That analysis is based on a very coarse first-guess and a limited number of observations and is likely unable to capture mesoscale features such as a sea breeze.

The PBL height fields for the 2 simulations are shown in Figure 29. The height field in the nudging simulation is smoother than that in the no-nudging simulation. This is most likely because the PBL height field is a reflection of the surface heating and upwards transfer of heat, moisture, and momentum. The nudging simulation smooths out the heat, moisture, and momentum fields within the PBL and doesn't allow the growth of the "plumes" seen in Runj and discussed previously in Section 7.3.

It is also interesting to note that the average PBL height (without the plumes) in the nudging simulation is similar to that in the no-nudging simulation. This is because the PBL height is primarily forced by the model and its PBL parameterization - not by any PBL height information in the grid analyses that are being nudged to. The grid analyses are based on very coarse first-guess information and any available observations. The only upper air observations used to improve the first-guess are the rawinsondes and they are only available at 0000 and 1200 UTC - as far as possible from 1800 UTC. In addition, the PBL varies enormously from 1200 UTC to 1800 UTC to 0000 UTC - for the continental U.S. the 0000 and 1200 UTC rawinsondes fall at the dusk/dawn PBL transitional time. If the PBL parameterization in the model does not predict a reasonable PBL height, it is unlikely that grid nudging will improve that estimate.

The temperature statistics shown in Figure 30-Figure 32 further illustrate these points. The temperature in the nudging simulation is better at night than in the no-nudging simulation but they are similar during the day. Likewise the wind speeds are better at night in the nudging simulation but similar or slightly worse during the day. The moisture statistics show that the no-nudging simulation is slightly better.

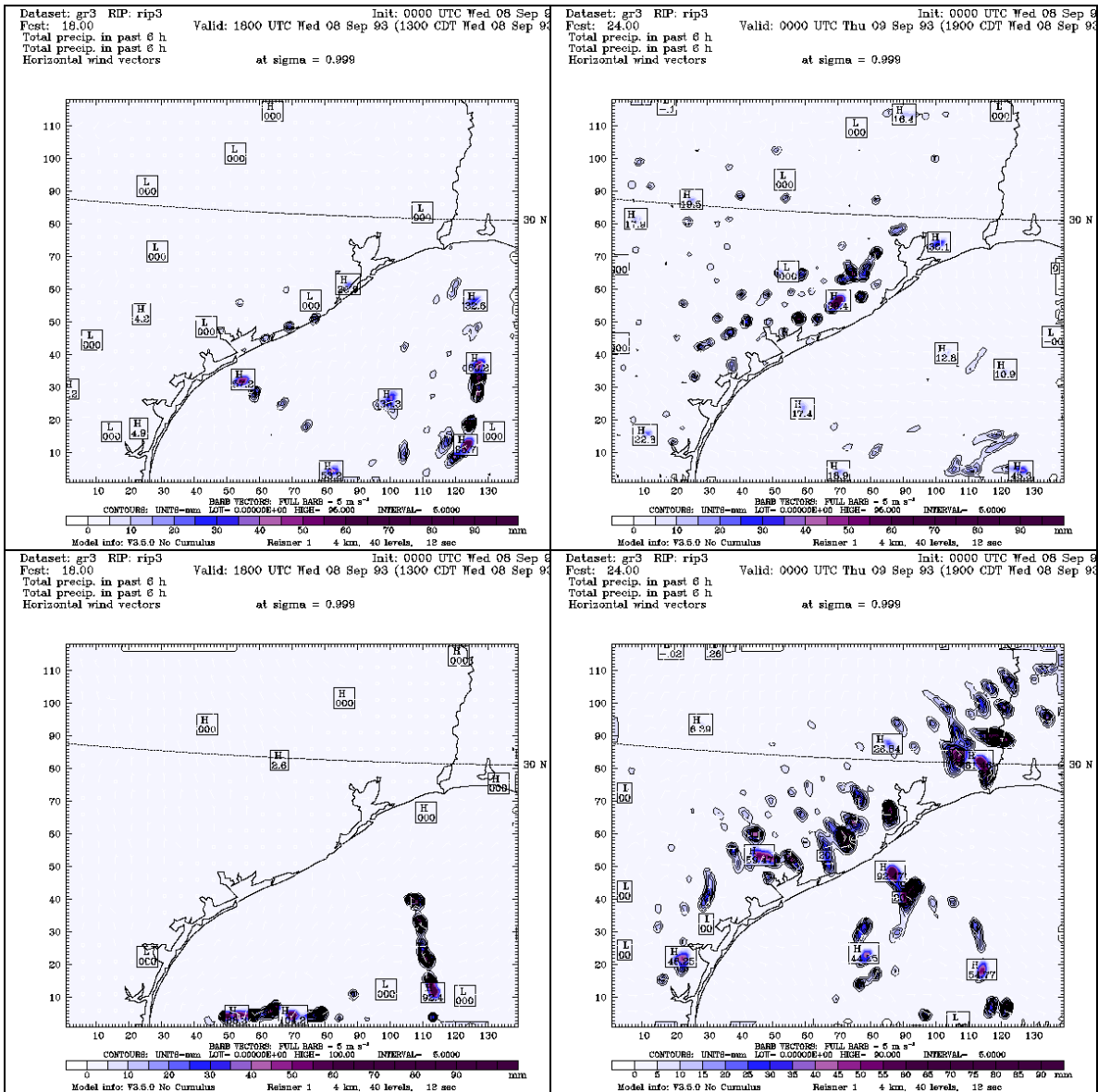


**Figure 27: 6 hr precipitation for a) Runj (no nudging) valid at 1800 UTC, b) Runj (no nudging) valid at 0000 UTC, c) Runo (grid nudging) valid at 1800 UTC, d) Runo (grid nudging) valid at 0000 UTC.**

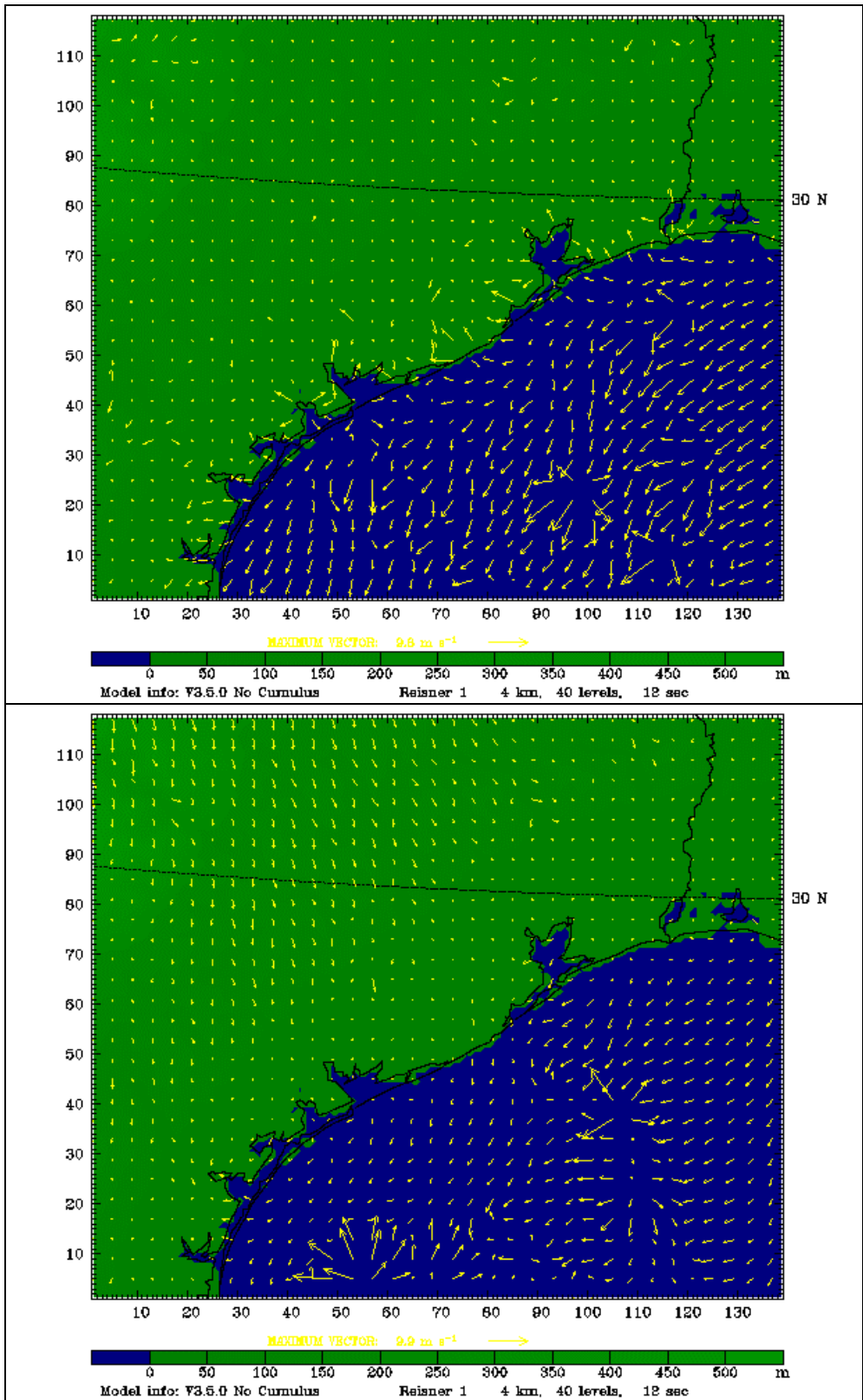


Figure 28 : Surface winds at 1800 UTC for a) Runj (no nudging) and b) Runo (grid nudging).

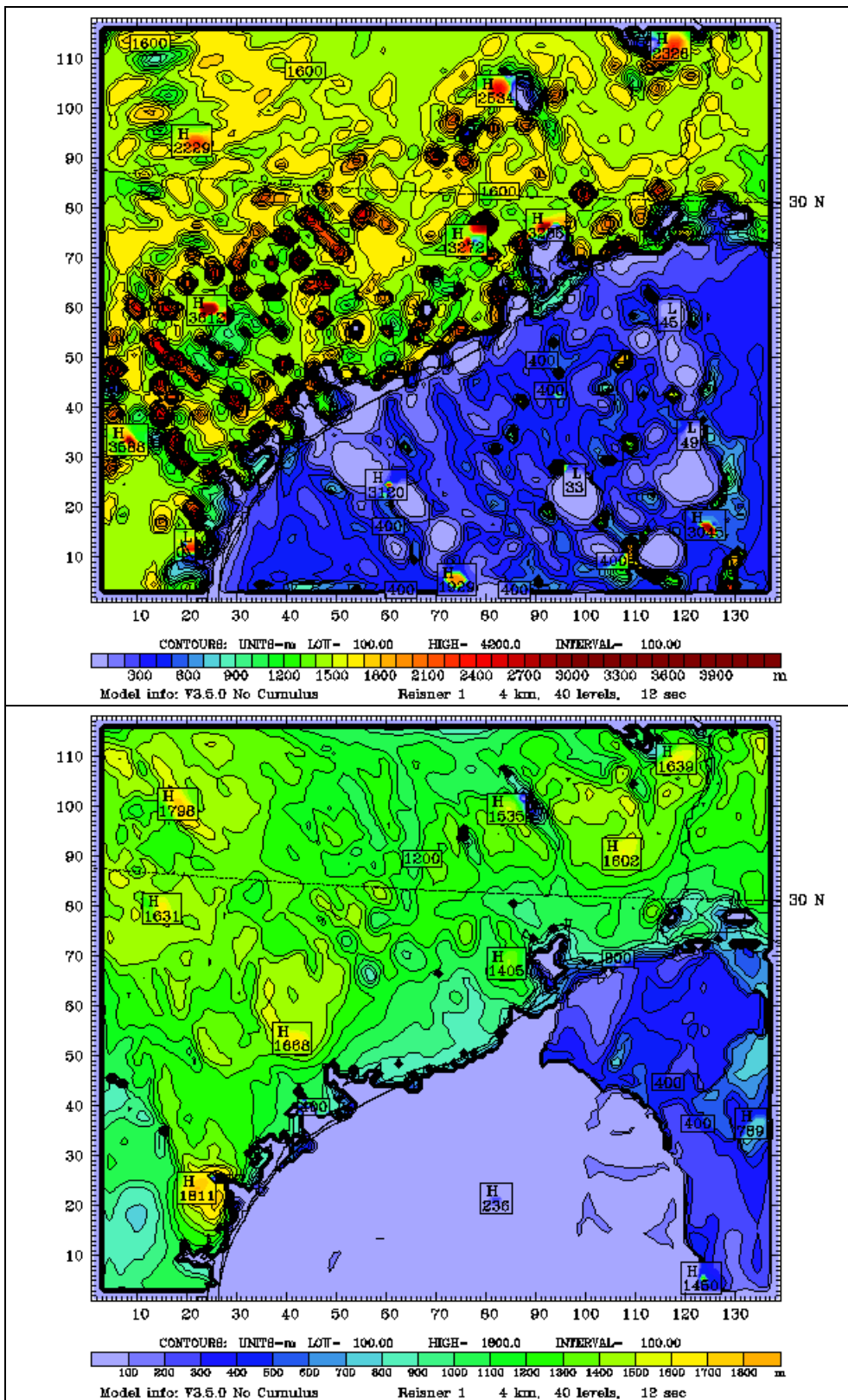
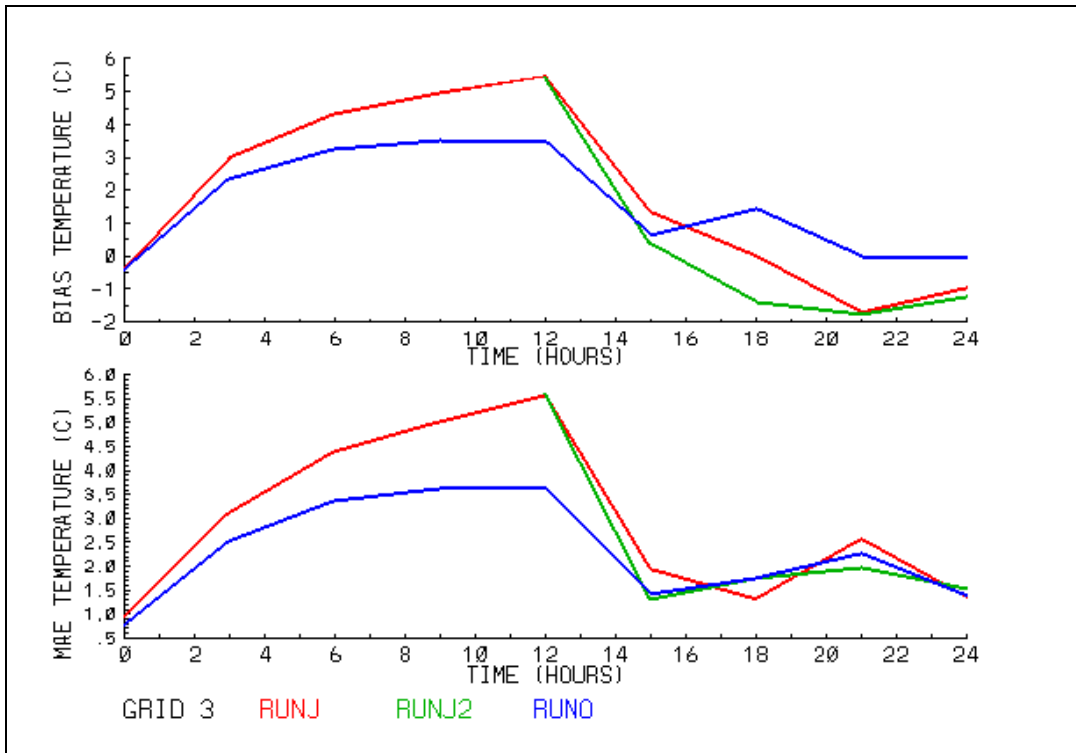
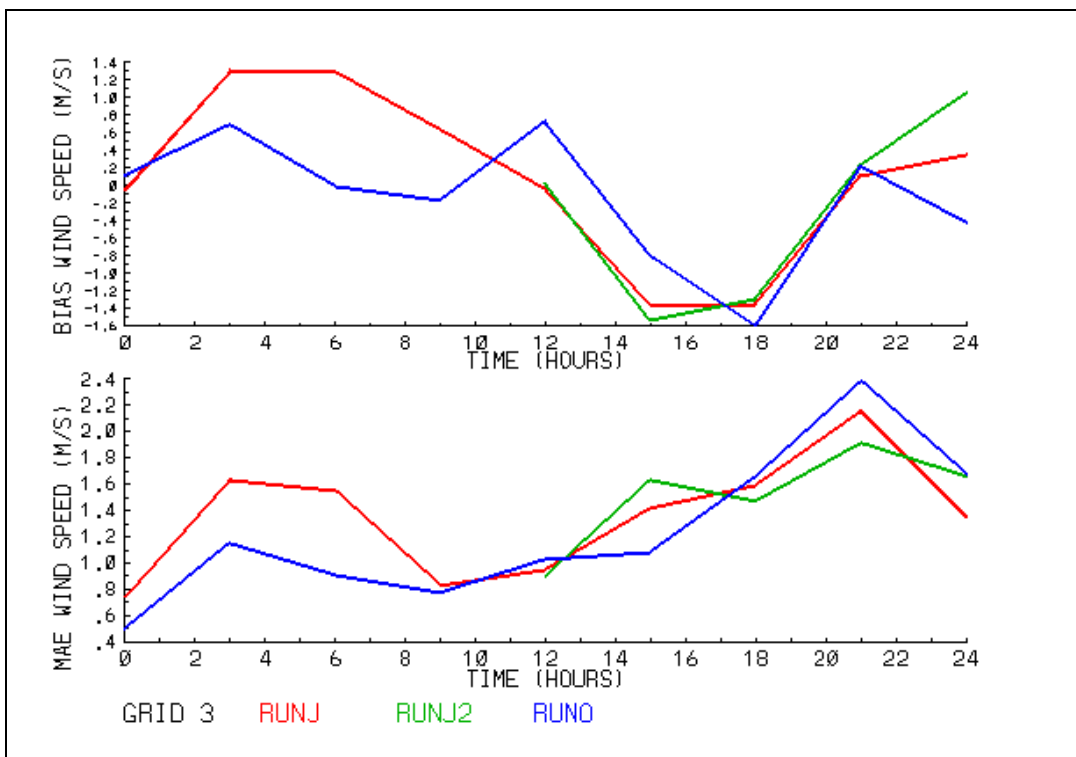


Figure 29 : Pbl height (m) at 1800 UTC 8 September for a) Runj (no nudging) and b) Runo (grid nudging).



**Figure 30 : Temperature statistics for domain 3 for the Runj (no nudging, red line), Runj2 (no nudging, modified GS PBL, green line), and Runo (nudging, blue line) simulations. Top graph is bias, bottom is MAE. The green curve runs from 12-24 hrs because the Runj2 simulation initialized grid 3 at 12 hrs.**



**Figure 31: Wind speed statistics for domain 3 for the Runj (no nudging, red line), Runj2 (no nudging, modified GS PBL, green line), and Runo (nudging, blue line) simulations. Top graph is bias, bottom is MAE. The green curve runs from 12-24 hrs because the Runj2 simulation initialized grid 3 at 12 hrs.**

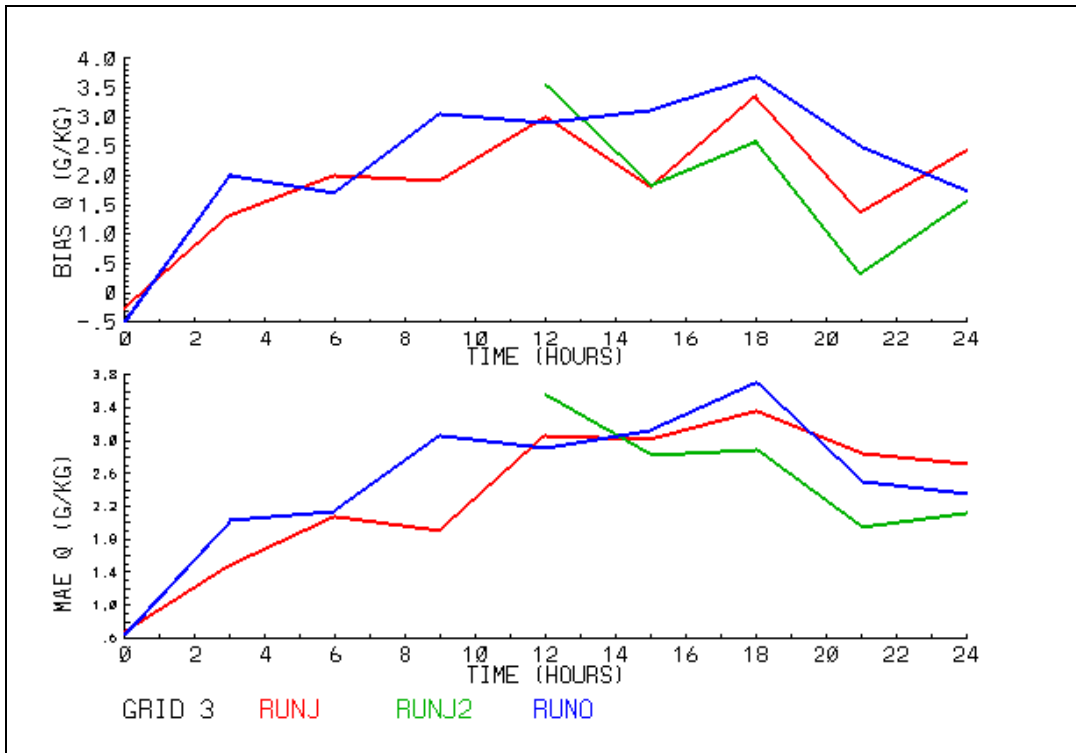


**Figure 32 : Specific humidity statistics for domain 3 for the Runj (no nudging, red line), Runj2 (no nudging, modified GS PBL, green line), and Runo (nudging, blue line) simulations. Top graph is bias, bottom is MAE. The green curve runs from 12-24 hrs because the Runj2 simulation initialized grid 3 at 12 hrs.**

## 7.6. Discussion of Sensitivity Results

The numerous sensitivity tests that were run have provided a very interesting look at the behavior of MM5 for the 8-9 September 1993 situation. Here, we will try to summarize the main issues of the runs as they relate to the undesirable features of the previous project's simulations.

### 7.6.1. Underprediction of surface wind speed

First, we will address the “easy” issues. The under-prediction bias for the surface wind speed is primarily controlled by the PBL scheme as it interacts with the land surface scheme. While we did not have time to attempt to use the newer landuse models that are available in newer versions of MM5 (since they needed different input datasets and are not widely used in the air quality community), the ETA MY PBL model did do a better job with maintaining a lower bias with the surface wind speed than the other PBL schemes. Other than that though, the ETA scheme had many of the same problems that plague the GS scheme, which we address below. Also, the implementation of the ETA scheme in the MM5 model does not include TKE advection, one of the main advantages of a prognostic TKE scheme as compared to other diagnostic subgrid schemes.

### 7.6.2. Lack of sea breeze circulations

The lack of good sea breeze development in the previous simulations was caused by a combination of three things: 1) estimating the sea surface temperature from the lowest

atmospheric level temperature, 2) the over-development of grid-scale convective cells whose cold surface outflow both overwhelmed and thermally suppressed any developing sea breeze circulations, and 3) using the FDDA analysis nudging through the entire depth of the atmosphere. For 1), this resulted in a sea surface temperature that was approximately 1C warmer than actually occurred, which led to a lower temperature difference between the land and ocean areas through the day as the air over the land warmed. This would reduce the thermal forcing for the sea breeze circulation and lead to a weaker pressure gradient force perpendicular to the coast. The FDDA further reduced the cross-coastal flow by nudging toward the data analysis. While there were numerous observing sites available, the grid analysis smoothed these out so that the data analysis produced a flow which was more parallel to the coast during the day, rather than perpendicular. It would be preferable to closely examine and “tune” the analyses used in the grid nudging, as well as some of the nudging parameters; there wasn’t time available for that in this project.

This is always a danger of performing any kind of FDDA, whether it be nudging to a gridded analysis or directly to observations. Even observational nudging needs to define a “radius of influence” around each individual observation. The “influence” of a particular observation is a user-specified parameter which is difficult to set and, in many places such as coastal areas and regions of complex terrain, is not a circular function as is assumed in many of the current observational nudging schemes. Some schemes do allow a wind-directed radial influence function (such as the Cressman banana scheme available in the MM5 pre-processing package) but even that could be less than optimal along a coastline – it might actually be preferable to extend the radius more perpendicular to the wind direction in such a case.

At smaller grid spacings, it is probably preferable to use observation nudging instead of analysis nudging because of both the increased importance of local mesoscale forcing and the increased irregularity of observation density on the smaller scales. Mountain/valley, land/water, and wet soil-/dry soil-forced circulations are all examples of mesoscale circulations that are predominant on smaller scales and the reason why mesoscale numerical models are valuable. An analysis based on a coarse first-guess and unevenly spaced observations will often not resolve these types of local scale circulations. When that analysis is used in a FDDA grid nudging scheme, the (correct) mesoscale-forced circulations that the model is trying to develop may be wiped out. In contrast, observation nudging can be applied more closely to where the observation is valid. However, even observation nudging in such instances can need extensive “tuning”. For instance, an observation on one side of a mountain range should probably not influence points close by but on the other side of the range.

This will be an even larger problem as the grid spacings for the meteorological and photochemical models continue to shrink. There are never enough observations to adequately define all of the important aspects of the meteorology that can be significant to the photochemistry. If there were adequate observations, the meteorological model would not be needed. Therefore, we stress here the importance of *assessing model performance without using FDDA* at all to verify that the meteorological model can adequately reproduce the important meteorology based on the physics of the situation. The purpose of the FDDA schemes is NOT to correct model errors, but to bring the model back toward the observations due to uncertainties in the model initialization,

surface characteristics, and lateral boundary conditions. The longer, multi-day simulations require FDDA due to the increasing effect of the uncertainties, but shorter term simulations should be able to perform adequately without FDDA, as is done on an operational basis when these same meteorological models are used in forecast mode. In addition, there are many aspects of the model simulation (PBL height for instance) that are not directly included in the observations, and may in fact evolve most strongly as a function of the model physics, independent of the FDDA analyses. This point was illustrated in the 3-grid FDDA tests. Proper simulation of such aspects can be crucial to the air quality and photochemical applications and yet is often dependent only on the model physics – not the FDDA.

### **7.6.3. Convective cells**

The more complicated problem that plagued the previous simulation was the generation and proliferation of deep convective cells. We had predicted that the cause was most likely the explicit cloud microphysical parameterization overemphasizing the effect of the latent heat release from shallower cumulus clouds. However, it turned out that microphysics were probably not the cause of occurrence of the convective cells. Rather it seems to be the PBL scheme, in conjunction with the MM5 non-hydrostatic scheme and the FDDA scheme, that caused these features apparent in both the previous and current simulations. Following is the trail of evidence that leads us to this conclusion.

As we started our sensitivity simulations of the 24 hour period, without any FDDA being used, we noticed the significant differences between the runs with the GS and the MRF scheme. The GS results showed numerous convective cells, some precipitating, some dry, that were mostly confined to the depth of the boundary layer. These are responsible for the spotty look to the results in Figure 15 of the PBL depth and other fields that we investigated, such as ground temperature. These “thermals” were very apparent in the GS and ETA results, but much weaker or non-existent in the MRF and Blackadar results.

These thermals brought back recollections of features seen in the RAMS model several years ago. We then looked in the MM5 results for one more clue and it was there. The TKE schemes had a significant super-adiabatic layer near the ground, especially in the GS scheme results. This super-adiabatic layer reached several degrees Celsius, stronger than normally seen in the real world.

The real world will reduce the magnitude of the super-adiabatic layer by creating thermals, but the real world can create thermals on any spatial scale. Generally the horizontal extent of the thermals will scale with the PBL depth. However, a model can only create circulations on the resolution of its grid. In these simulations with the 4 km grid, the thermals during the morning should be subgrid-scale, and therefore the PBL scheme should handle the reduction of the superadiabatic layer. But if the PBL scheme does not mix the heat near the ground up adequately, it can lead to another chain of events in a non-hydrostatic model.

This chain of events can occur when the depth of a circulation becomes of similar magnitude as the horizontal grid spacing. The non-hydrostatic models are based on an equation set which contains a buoyancy term that is formulated with a temperature perturbation from a base state. When the superadiabatic layer first forms in the morning,

vertical motion is forced upward with a positive acceleration from the buoyancy term. However, the vertical circulation is limited by two factors as the air rises: 1) it will cool adiabatically and soon be colder than the surrounding air and, 2) the pressure near the ground will become lower. If there is not compensating horizontal divergence, the pressure gradient force will be directed downward. And because of the differences between the horizontal and vertical grid spacings, it takes longer for the horizontal direction to respond to the lower pressure.

But as the morning progresses, the subgrid-scale scheme will mix some heat upward, creating a deeper mixed layer. Now, a parcel from the superadiabatic layer near the ground is better able to travel vertically. As the depth of the neutral layer approaches that of the horizontal grid spacing, the model is more able to create the compensating horizontal convergence, which in turn removes any inhibition the vertical circulation has to develop. Thus, the grid-scale thermals are created, but at a much larger scale than they should be.

It is probable that this is the cause of the thermal-like, convective circulations. This is also the reason for our test of the GS scheme where we multiplied the vertical eddy heat diffusivities by a factor of 5. By allowing the subgrid scheme to reduce the magnitude of the super-adiabatic layer, the resolvable-scale buoyancy term was reduced, which in turn significantly reduced the number and strength of the resolved thermals. This is also why the diagnostic PBL schemes did not exhibit these features. The Blackadar scheme requires that a neutral layer be maintained, which doesn't allow a superadiabatic layer to be formed at all, while the MRF scheme prescribes a vertical eddy diffusivity profile which removed the superadiabatic layer much better than the TKE schemes.

Note that a hydrostatic model will not have the capacity to develop these types of thermals, since the hydrostatic equation set doesn't have a buoyancy term to start this chain of events. Also, a non-hydrostatic model in a hydrostatic configuration (where the horizontal grid spacing is much larger than the vertical extent of a circulation) will not develop these either, since the compensating horizontal convergence can't occur.

Now the question is: How are these thermals, which were mostly confined to the boundary layer, related to the deep convection of the previous simulations? The answer is related to the FDDA scheme. The analysis grid nudging scheme acts as a horizontal filter. What a filter does is to effectively increase the horizontal grid spacing, thus changing the horizontal scale at which circulations can occur. Therefore, as is evidenced by Figure 29, the horizontal scale was increased enough so that the thermals were not able to be created.

But as the day goes on into the afternoon, the boundary layer will continue to grow to the point where it will be close enough to the new filtered horizontal spacing. The vertical extent of the circulation can again get deep enough, perhaps to the point where significant condensation can occur, which further enhances the vertical extent. And because of the larger horizontal extent due to the filtering, if the horizontal compensation occurs, it can create the deep convection that was evident in the previous runs. Figure 33 shows the surface wind field from Runo, the nudged GS run, which clearly shows the outflow from deep convective cells which were formed later in the afternoon. Note also Figure 4b,

where it is clear that the thermals were created on the nested 1.3 km grid in the previous run, even though they were not formed on the 4 km grid.

Dataset: gr3 RIP: rip3 Init: 0000 UTC Wed 08 Sep 93  
 Fcst: 24.00 Valid: 0000 UTC Thu 09 Sep 93 (1900 CDT Wed 08 Sep 93)  
 Terrain height AMSL  
 Horizontal wind vectors at sigma = 0.999

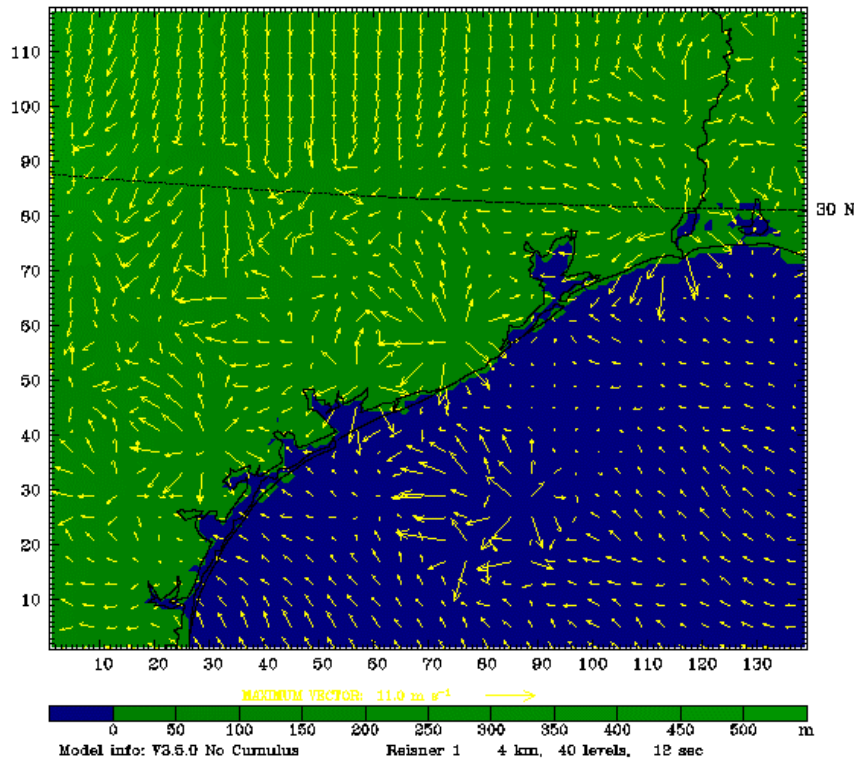


Figure 33: Surface winds at 9 September 0000 UTC for Runo (grid nudging).

This same issue is consistent with what other MM5 users are finding in their simulations. The following excerpt is taken from: *TNRCC Air Quality Modeling Advanced Texas Air Quality Model: Study, Progress, Results by MCNC* concerning their simulations of this same case:

---

MCNC ran the 36km and 12km sets of runs with MM5V2.12-GSPBL without difficulty, completing those runs in late January of 2000. However, the 04km runs proved different - - within the first 12-simulation hours, the model crashed in GSPBL. The crash occurred when the TKE values exceeded a critical value at model top (100mb), indicating that at high-resolution, the parameterization was not damping TKE near the tropopause.

Significant energy was then directed toward determining why, including numerous discussions with Penn State (Seaman and Stauffer). The crash occurred in a **grid-resolved** deep-convective cloud where vertical velocities were quite high and turbulence generation is efficient above the surface-based PBL. Since GSPBL models turbulence through the depth of the atmosphere (and not just the PBL), this was notably an instance of free-tropospheric failure.

After noting that other groups and projects were encountering similar failures, it was finally determined that the only viable way to overcome the problem was to place the model top clearly in the stratosphere (at 50mb for example) AND provide an isothermal reference temperature profile above the tropopause. This would have the effect of naturally damping the vertical growth of deep convection and shutting down turbulence production near the top of grid-resolved deep convective clouds. In order to do this efficiently, we would have to move to version 3 of MM5, since the isothermal reference atmosphere in the stratosphere had now been built into version 3.

By this time, however, the run-production schedule for ATAQM-DC was slipping, and project funds would not permit a full implementation of Version 3 of the model.

Hence, in consultation with TNRCC, the decision was made to use the less-sophisticated MRF PBL scheme, which is a non-local scheme based on a reference K-profile.

---

So to summarize, the chain of events that causes the thermals, and in some cases the erroneous deep convection, is brought on by the inability of the PBL scheme to adequately mix heat upward from the lower boundary layer. The buoyancy produced by the heat excess produces buoyant effects in the non-hydrostatic scheme which then can cause thermals to form at the grid scale, a much larger scale than they would have formed at in reality.

Thus, we arrived at the same conclusion as MCNC and chose also to use the MRF PBL scheme, even with its recognized deficiencies, for the complete episode 4-grid runs. We recommend that the GS scheme should not be used, especially at higher resolution, without further testing, both of near-ground effects and also the behavior with resolved convective clouds. We also recommend significant basic testing of the MM5 non-hydrostatic scheme itself, especially in simulations where significant non-hydrostatic effects are expected to occur. Based on our long experience with non-hydrostatic models, we feel there is a possibility that the MM5 non-hydrostatic scheme is exaggerating the effect of vertical accelerations.

## **8. New 4 grid simulations**

Based on the above results of the sensitivity tests, we decided to use the MRF PBL, KF2 cumulus parameterization, and Reisner 1 microphysics schemes in the 4-grid nudging simulation. Although the statistical results associated with the ETA MY PBL were promising, that scheme (and also the GS MY PBL scheme) produced what we considered too-low PBL heights during the day. In addition, there was the increased frequency of grid-scale thermals and convection on the smaller scales associated with the use of the GS and ETA MY schemes.

In the previous project's 4-grid simulation (Runorig4), both surface and upper air nudging was done for all 4 variables (T, q, u, and v) on all grids. The MM5 nudging scheme uses a surface analysis for nudging within the PBL in unstable regimes and uses the upper air analysis for the nudging above that. Within the scheme, all 4 variables from the surface analysis are nudged upward throughout the PBL. This is problematic for temperature nudging and the MM5 documentation does in fact recommend against temperature nudging within the PBL. We decided to not use boundary layer nudging at

---

all in these 4-grid simulations, both because of the worrisome formulation and because it would tend to diffuse or wash out the developing sea breeze circulation. The MM5 options we thus used were no-surface/boundary-layer-nudging and setting inonpbl=1 for all 4 grids and all 4 variables.

The Runnew4 simulation was run with 3 grids from 0000 UTC 6 September through 0000 UTC 8 September. Domain 4 was then initialized at 0000 UTC 8 September and all 4 domains were integrated through 0600 UTC 12 September. Grid nudging above the boundary layer was performed on all domains throughout the simulation.

Figure34 shows the grid 4 surface winds at 1800 UTC 8 September and 0000 UTC 9 September for both the Runorig4 and Runnew4 simulations. The sea breeze in the Runnew4 simulation is nicely developed as contrasted with the Runorig4 results at this time.

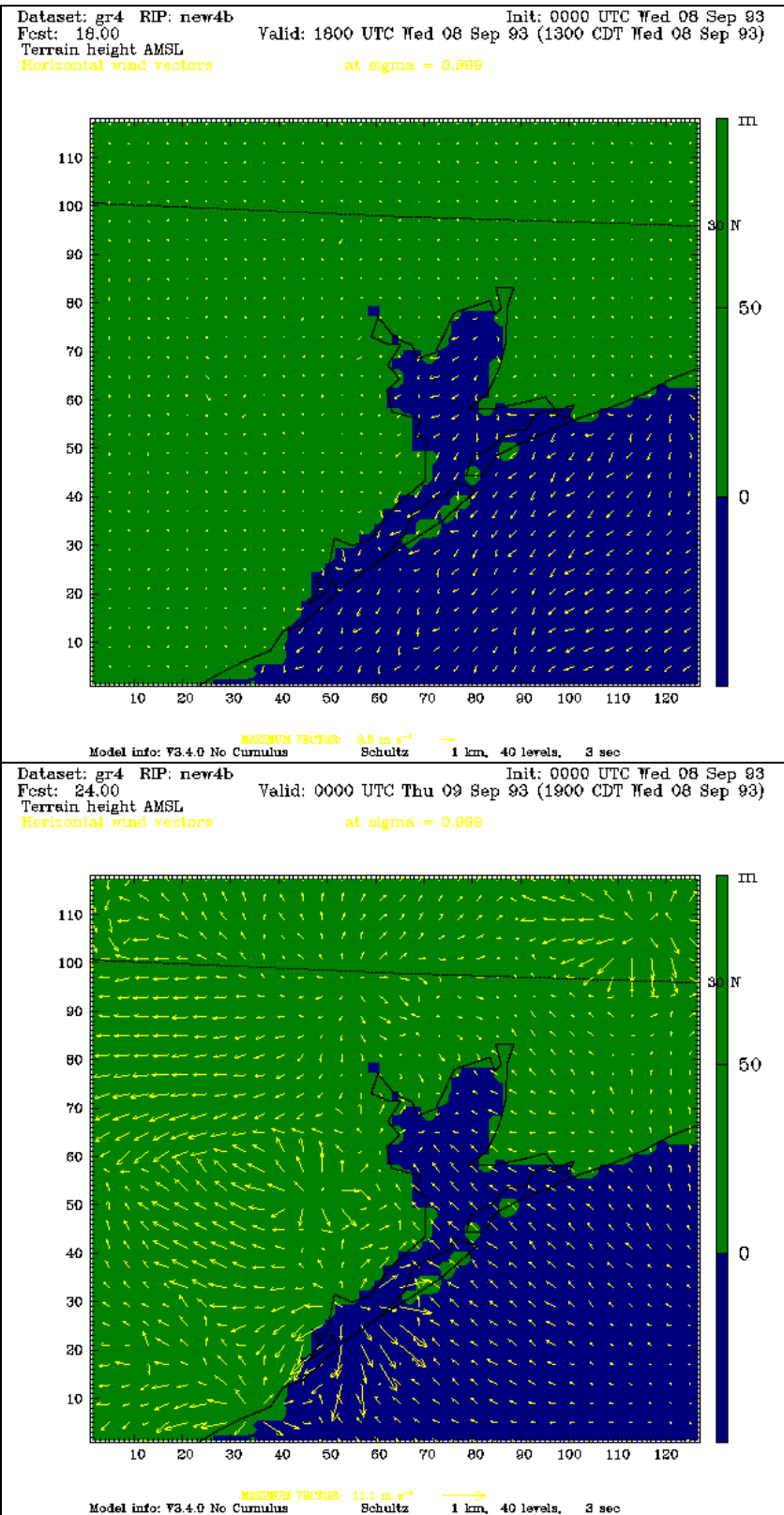
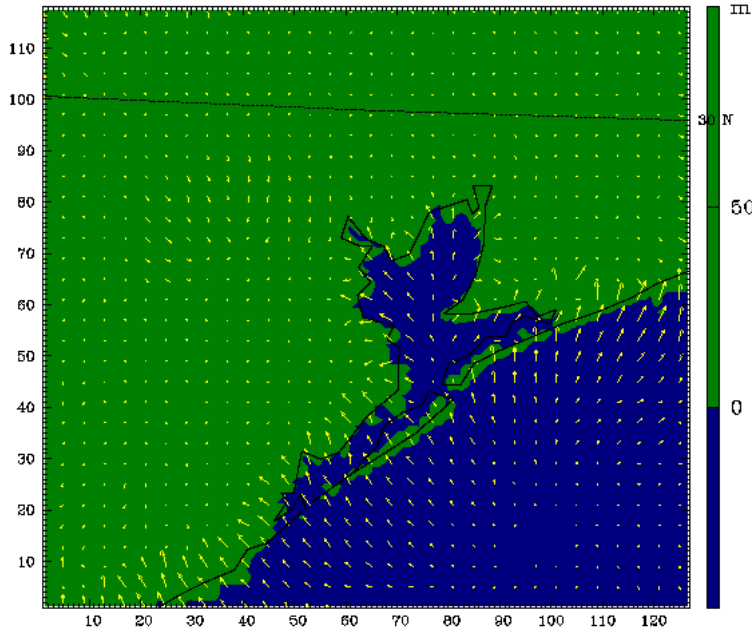


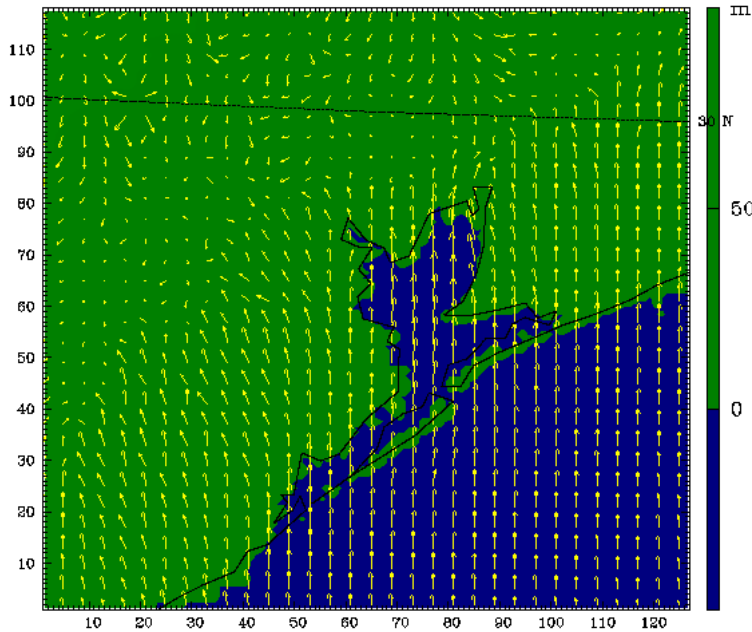
Figure 34 : Surface winds on grid 4 at a) 1800 UTC 8 September for Runorig4, b) 0000 UTC 9 September for Runorig4, c) 1800 UTC 8 September for Runnew4, b) 0000 UTC 9 September for Runnew4.

Dataset: gr4 RIP: new4b Init: 0000 UTC Mon 06 Sep 93  
 Fcst: 66.00 Valid: 1800 UTC Wed 08 Sep 93 (1300 CDT Wed 08 Sep 93)  
 Terrain height AMSL  
 Horizontal wind vectors at sigma = 0.999



Model info: V3.5.0 No Cumulus MRF PBL Reissner 1 1 km, 40 levels, 4 sec

Dataset: gr4 RIP: new4b Init: 0000 UTC Mon 06 Sep 93  
 Fcst: 72.00 Valid: 0000 UTC Thu 09 Sep 93 (1900 CDT Wed 08 Sep 93)  
 Terrain height AMSL  
 Horizontal wind vectors at sigma = 0.999



Model info: V3.5.0 No Cumulus MRF PBL Reissner 1 1 km, 40 levels, 4 sec

Figure 34: Concluded.

The statistics comparing Runorig4 and Runnew4 on domain4 are shown in Figure 35- Figure 37. Runnew4 compares favorably with Runorig4 in the first 36 hrs but deteriorates after that. Closer examination of the Runnew4 simulation revealed that a large convective cell developed at the south-east corner of grid 4 around 1200 UTC 9 September and was almost continuously active and present in domain 4 after that. The radar summaries over that time period show scattered convection in the region throughout the period and an increase in convection around 10 September especially, but nothing with the consistency and duration of the convection that developed in the model. The effect of this convection is clearly seen in the statistics: a cold bias in the surface temperatures due to outflow and a suppression and swamping of any sea breeze development. Figure 38 shows the surface temperatures and winds in the Runnew4 simulation at 1800 UTC 9 September – the effects of the rogue convection are clearly illustrated.

The convection that caused a problem in the Runnew4 simulation seemed to start exactly at the south-east corner of grid 4, as shown in Figure 39. We speculated that the convection could have been initiated by a model grid discontinuity between the nests; grid nest boundary placement and noise is sometimes a factor in nested grid simulations. To test this theory, we ran a 3-grid-only simulation (Runnew3) over the same period and compared the results to the grid 3 results from Runnew4. The convection did not develop at that location and time in Runnew3, but strong convection did develop later in that simulation on 10 September. However, the radar summaries do show some strong convection over the Texas coast on that day. The statistics comparing grid 3 from Runnew4 and Runnew3 are shown in Figure 40-Figure 442.

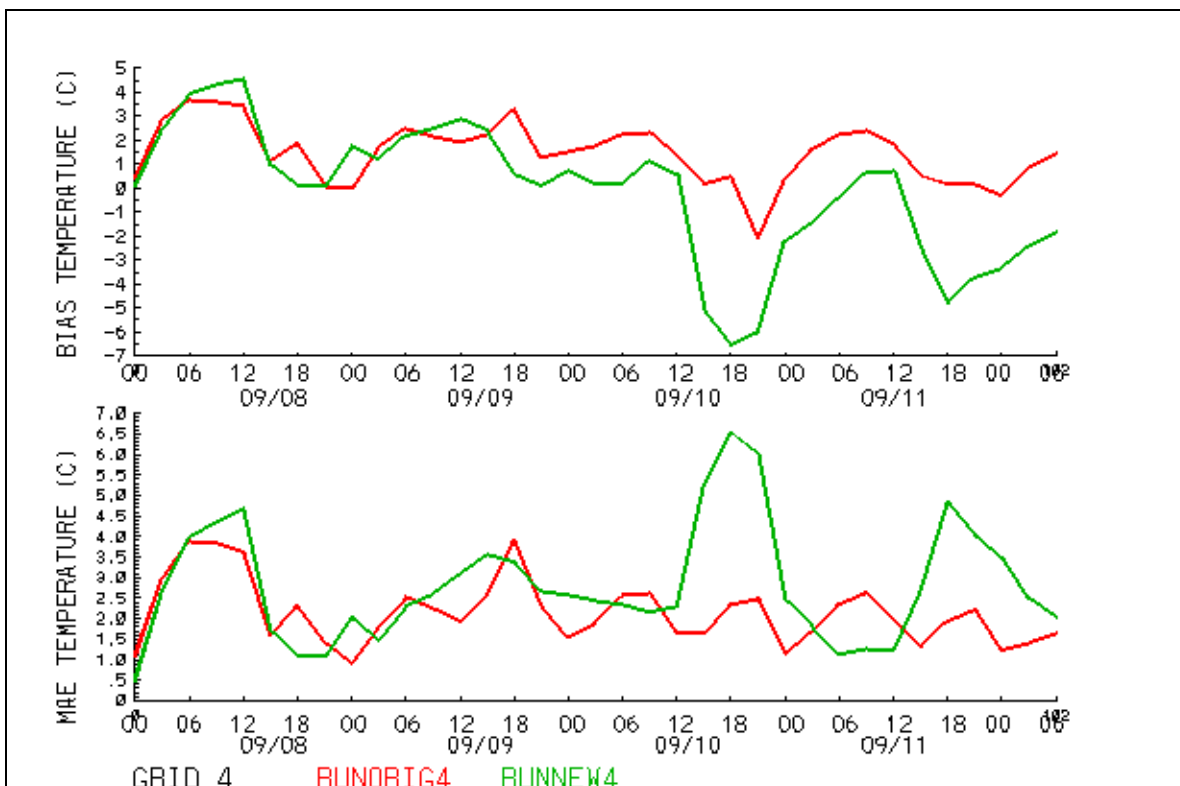


**Figure 35 : Temperature statistics over domain 4 from 0000 UTC 8 September through 0600 UTC 12 September for the Runorig4 (red line) and Runnew4 (green line) simulations.**

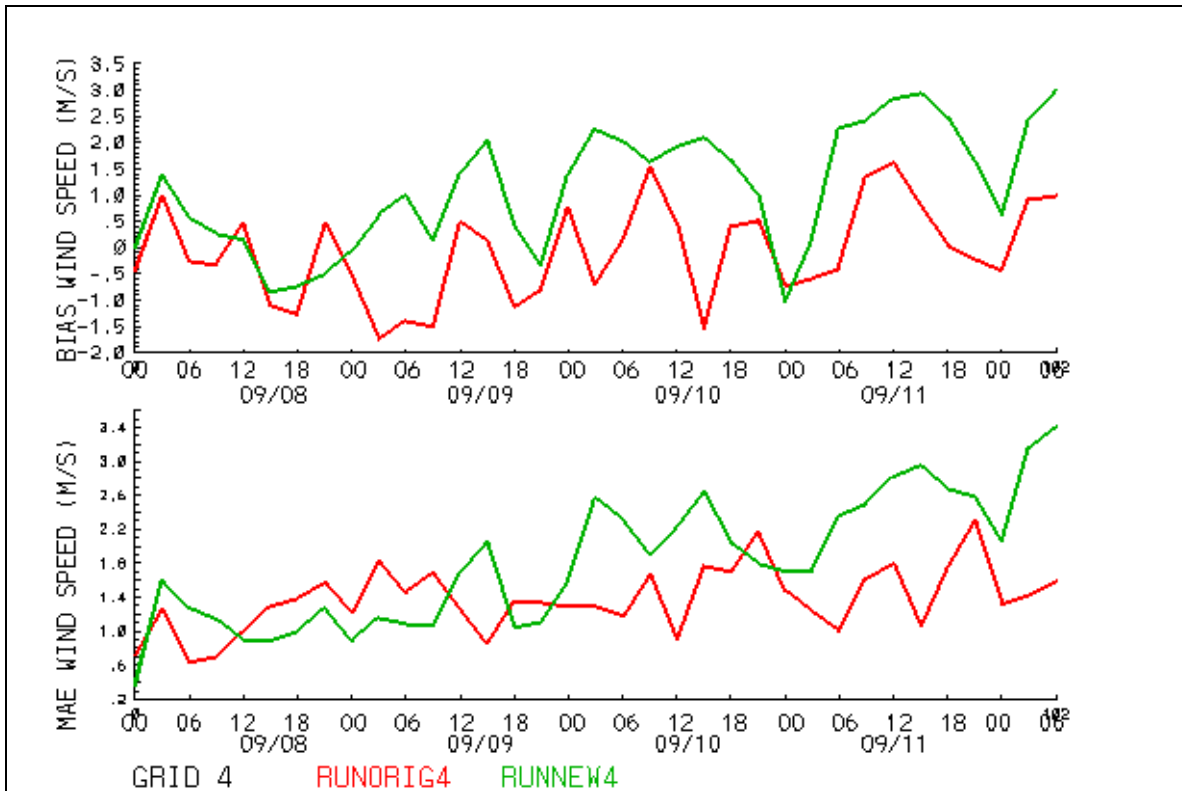


**Figure 36 : Wind speed statistics over domain 4 from 0000 UTC 8 September through 0600 UTC 12 September for the Runorig4 (red line) and Runnew4 (green line) simulations.**

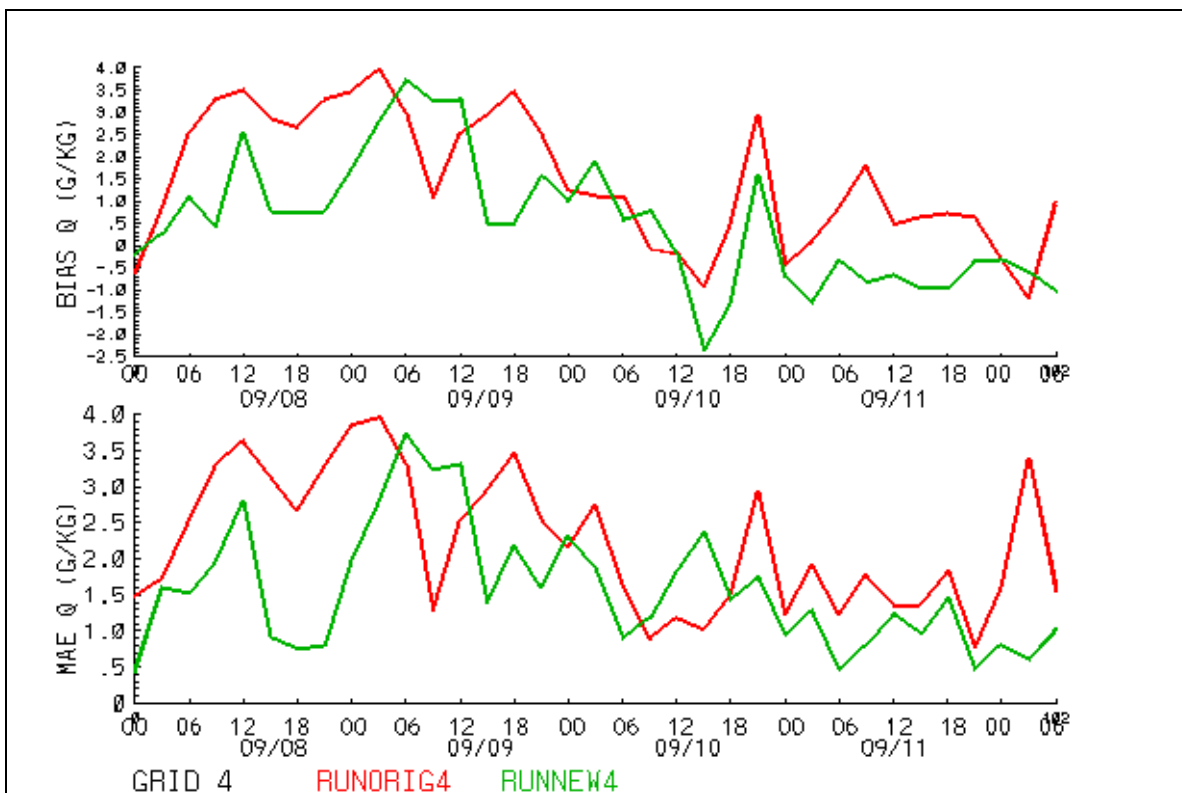


**Figure 37 : Specific humidity statistics over domain 4 from 0000 UTC 8 September through 0600 UTC 12 September for the Runorig4 (red line) and Runnew4 (green line) simulations.**

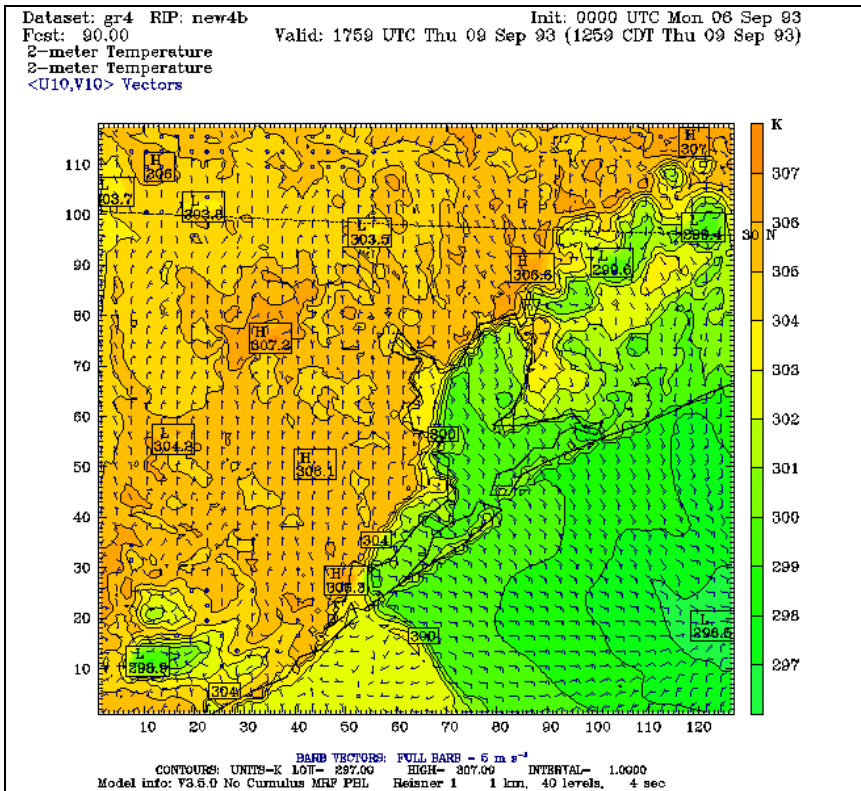


**Figure 38 : Surface temperature and winds over domain 4 in the Runnew4 simulation at 1800 UTC 9 September.**

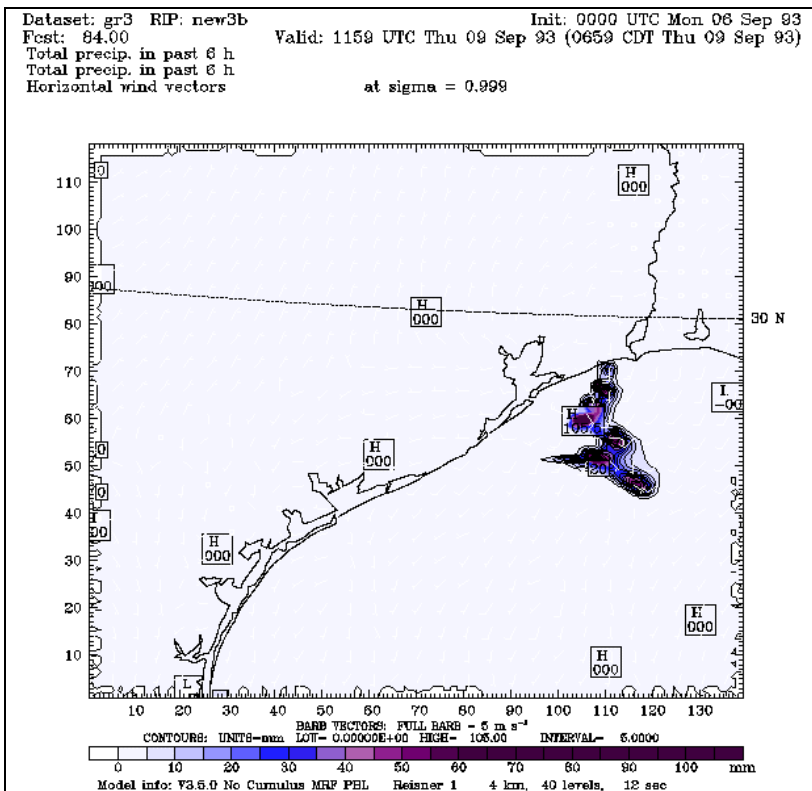


**Figure 39 : 6 hr precipitation over domain 3 in the Runnew4 simulation at 1200 UTC 9 September. Note how the precipitation has started over the south-east corner of the grid 4 boundaries.**

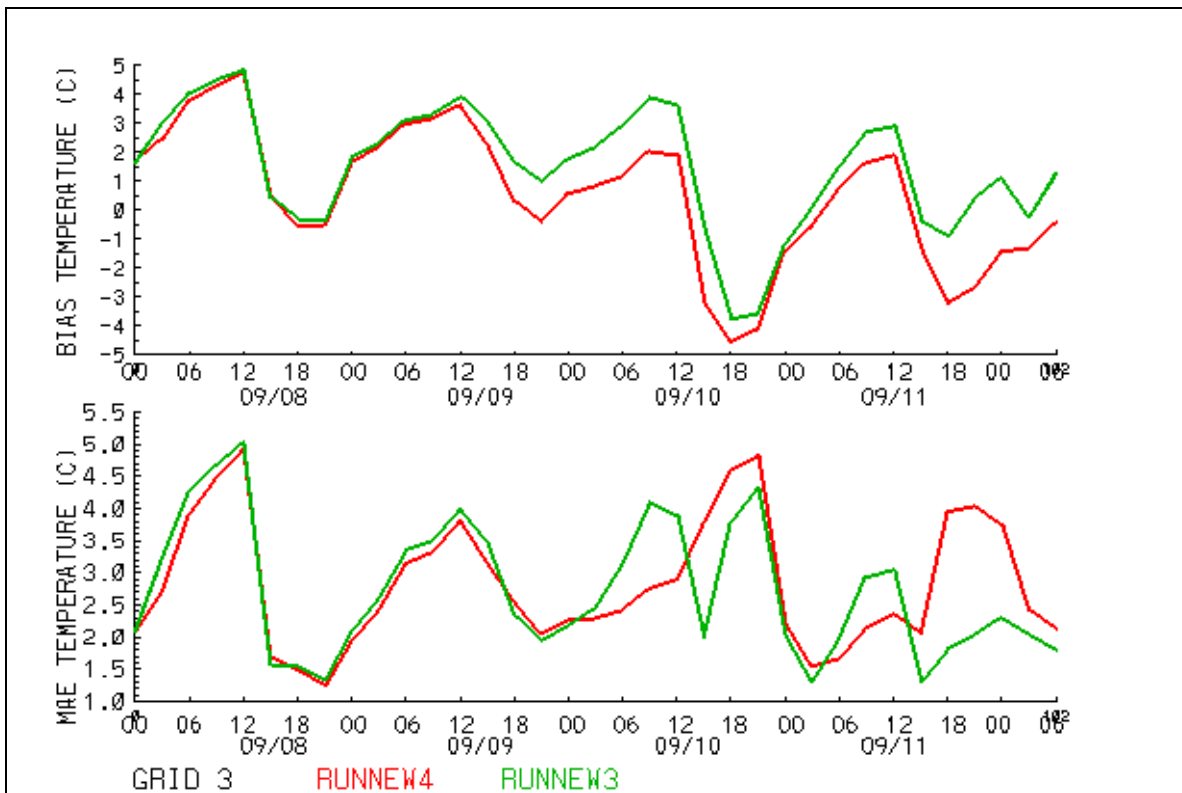


**Figure 40 : Temperature statistics over domain 3 from 0000 UTC 8 September through 0600 UTC 12 September for the Runnew4 (red line) and Runnew3 (green line) simulations.**

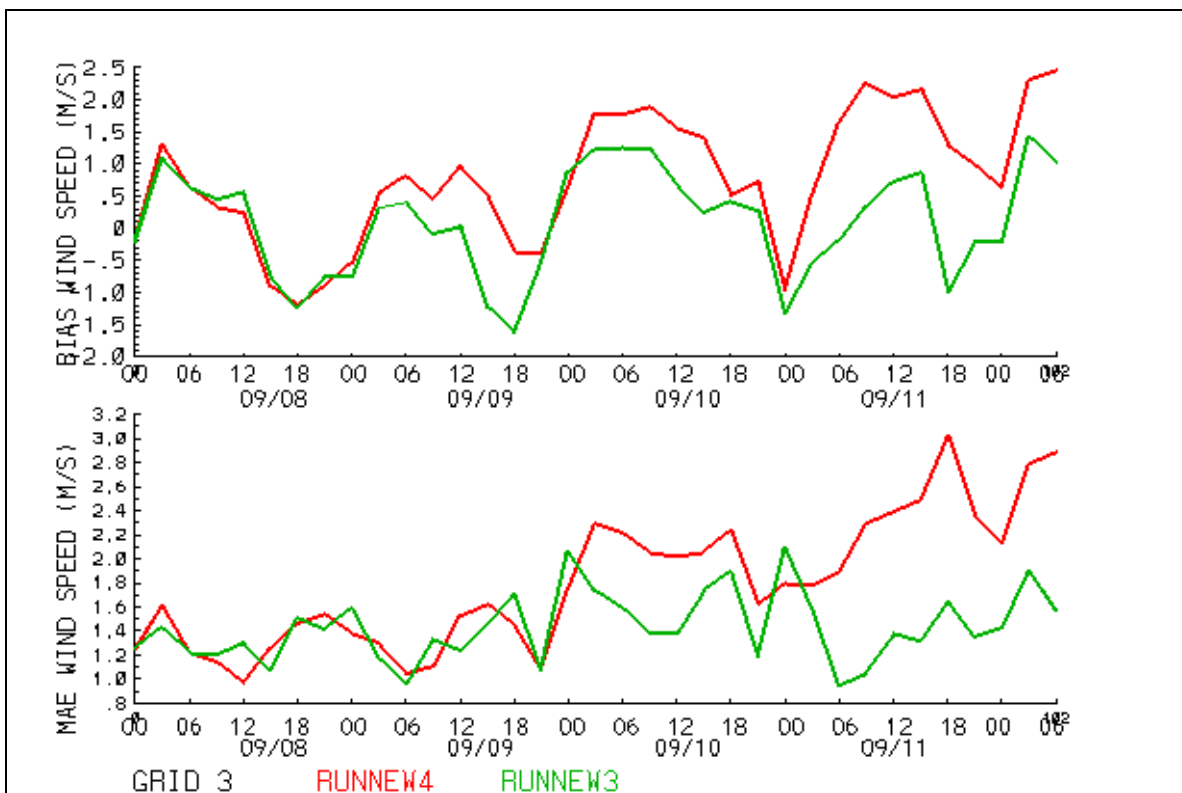


**Figure 41: Wind speed statistics over domain 3 from 0000 UTC 8 September through 0600 UTC 12 September for the Runnew4 (red line) and Runnew3 (green line) simulations.**

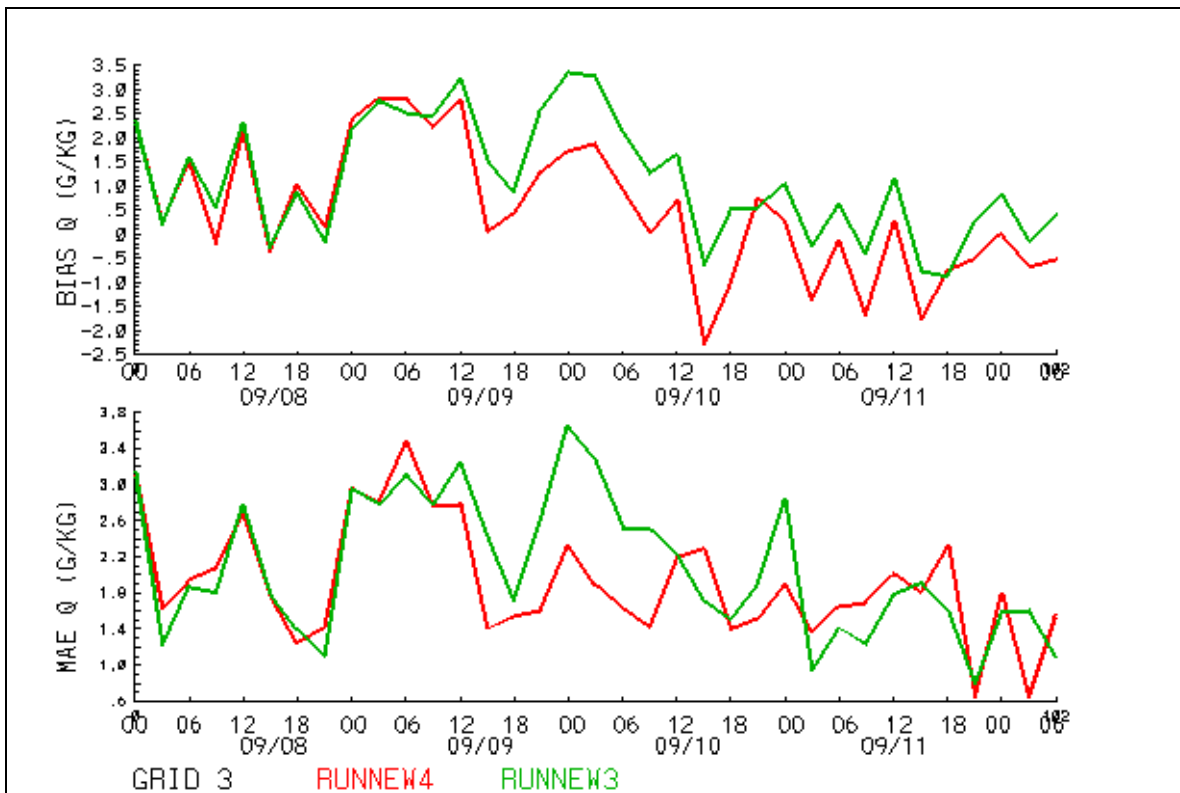


**Figure 42 : Specific Humidity statistics over domain 3 from 0000 UTC 8 September through 0600 UTC 12 September for the Runnew4 (red line) and Runnew3 (green line) simulations.**

A final simulation, Runnew4b, was done with a modification to the grid nudging scheme as suggested by ENVIRON. Other than the nudging modification, the simulation was configured exactly the same as the Runnew4 simulation and used the same data sets. For the Runnew4b simulation the upper air nudging was only implemented above the sigma=0.85 level in the model atmosphere (level 27 in this configuration). As in the Runnew4 simulation, the surface/boundary layer nudging was turned off. The results from this simulation were only slightly different from those of the Runnew4 simulation. The surface winds at 1800 UTC 8 September and 0000 UTC 9 September are shown in Figure 43 and are very similar to those from the Runnew4 simulation shown in Figure 34c and Figure 34d; the sea breeze in both simulations developed nicely through this period. Figure 38 and Figure 44 show the surface temperature and winds in the Runnew4 and Runnew4b simulations at 1800 UTC 9 September – the over-developed convection is apparent in the Runnew4b simulation also, although slightly delayed from the Runnew4 simulation. Finally, the temperature, wind speed and specific humidity statistics comparing the Runnew4, Runorig4 and Runnew4b simulations on grid 4 are shown in Figure 45-Figure 47. Again, the Runnew4 and Runnew4b performances are very similar.

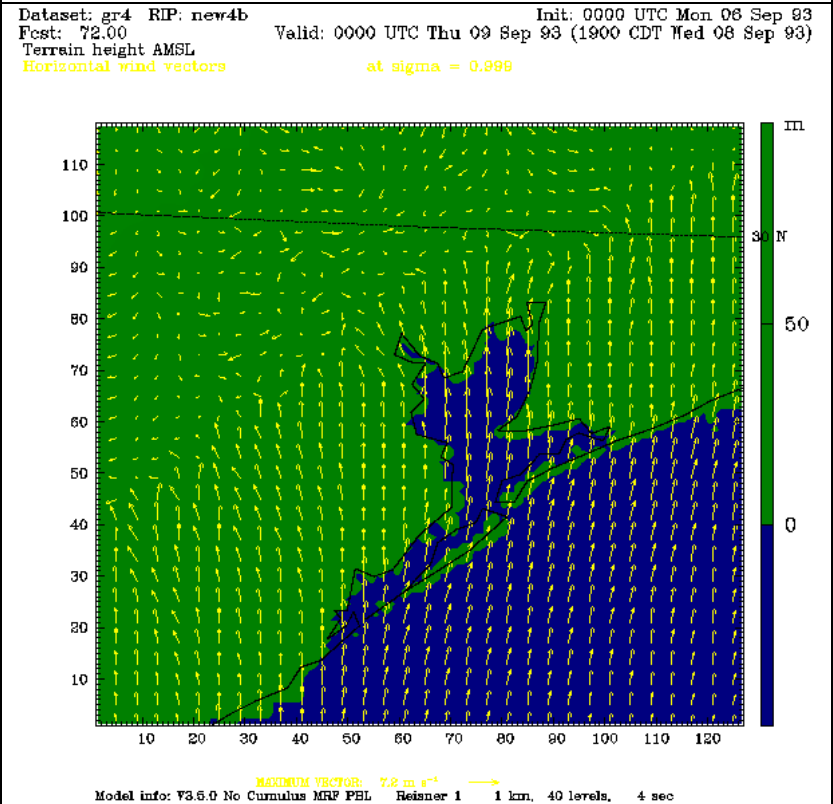
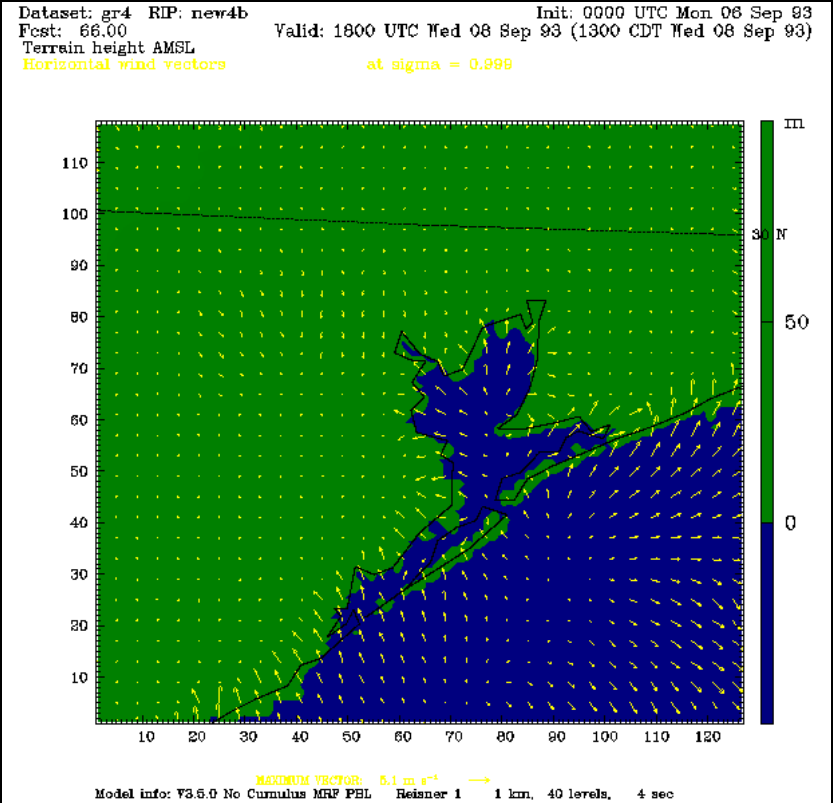


Figure 43 : Surface winds on grid 4 at a) 1800 UTC 8 September for Runnew4b, b) 0000 UTC 9 September for Runnew4b.

Dataset: gr4 RIP: new4b  
Fest: 90.00  
2-meter Temperature  
2-meter Temperature  
<U10,V10> Vectors

Init: 0000 UTC Mon 06 Sep 93  
Valid: 1759 UTC Thu 09 Sep 93 (1259 CDT Thu 09 Sep 93)

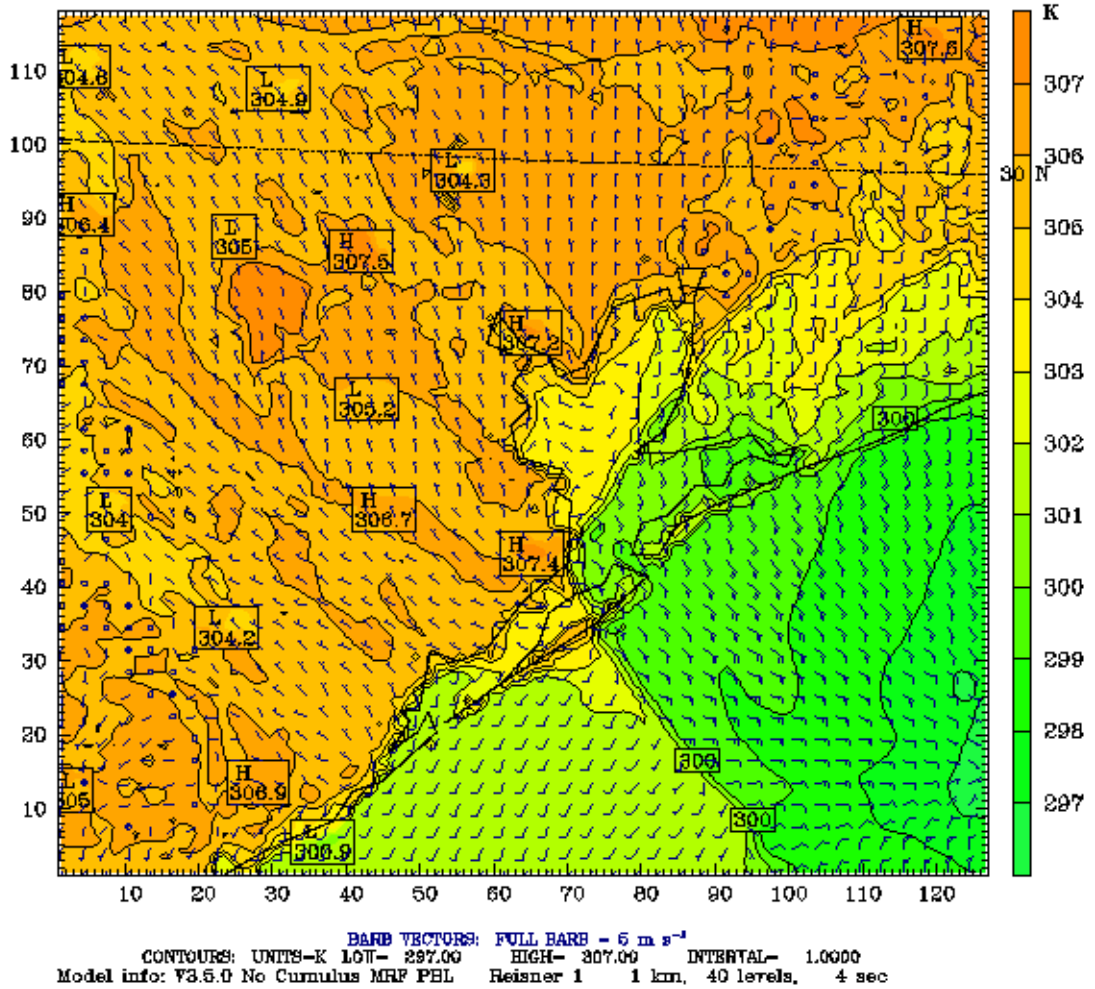
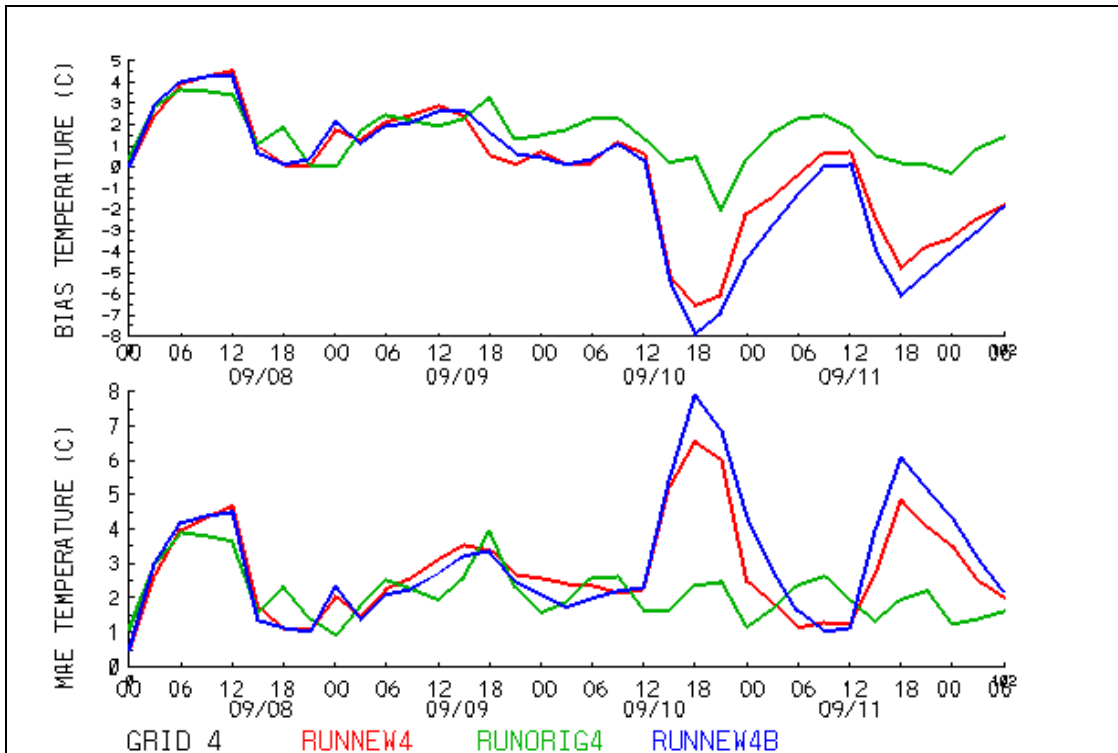
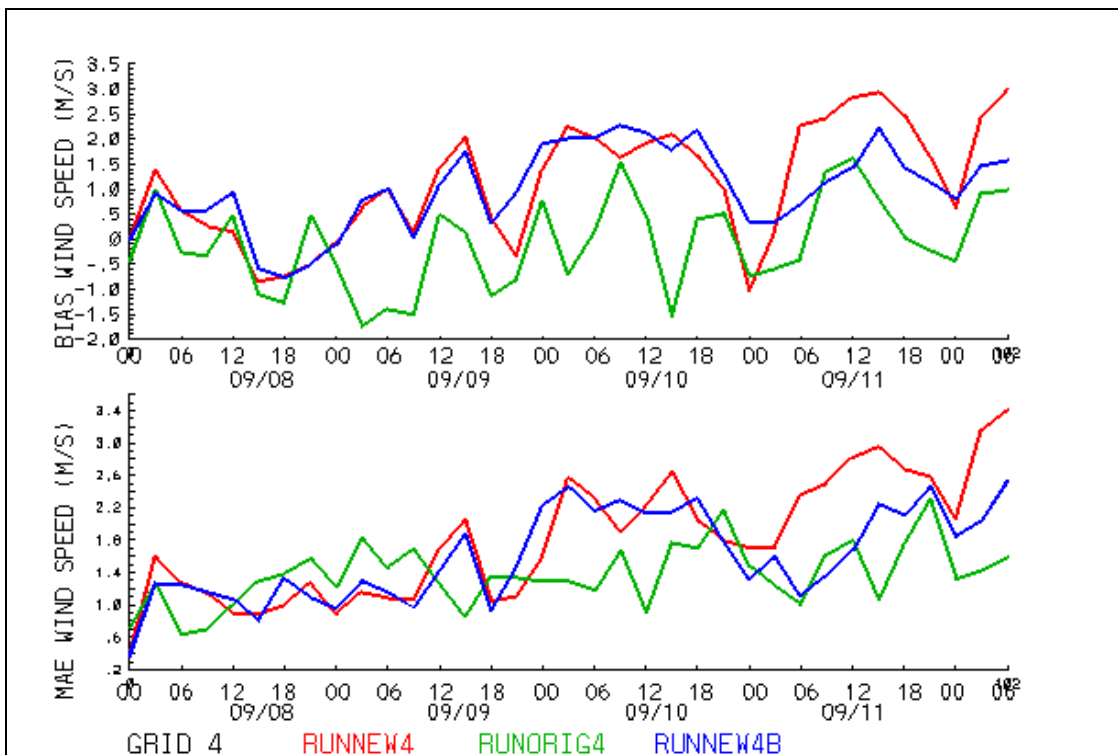


Figure 44: Surface temperature and winds over domain 4 in the Runnew4b simulation at 1800 UTC 9 September.



**Figure 45 : Temperature statistics over domain 4 from 0000 UTC 8 September through 0600 UTC 12 September for the Runnew4 (red line), Runorig4 (green line), and Runnew4b (blue line) simulations.**



**Figure 46 : Wind speed statistics over domain 4 from 0000 UTC 8 September through 0600 UTC 12 September for the Runnew4 (red line), Runorig4 (green line), and Runnew4b (blue line) simulations.**

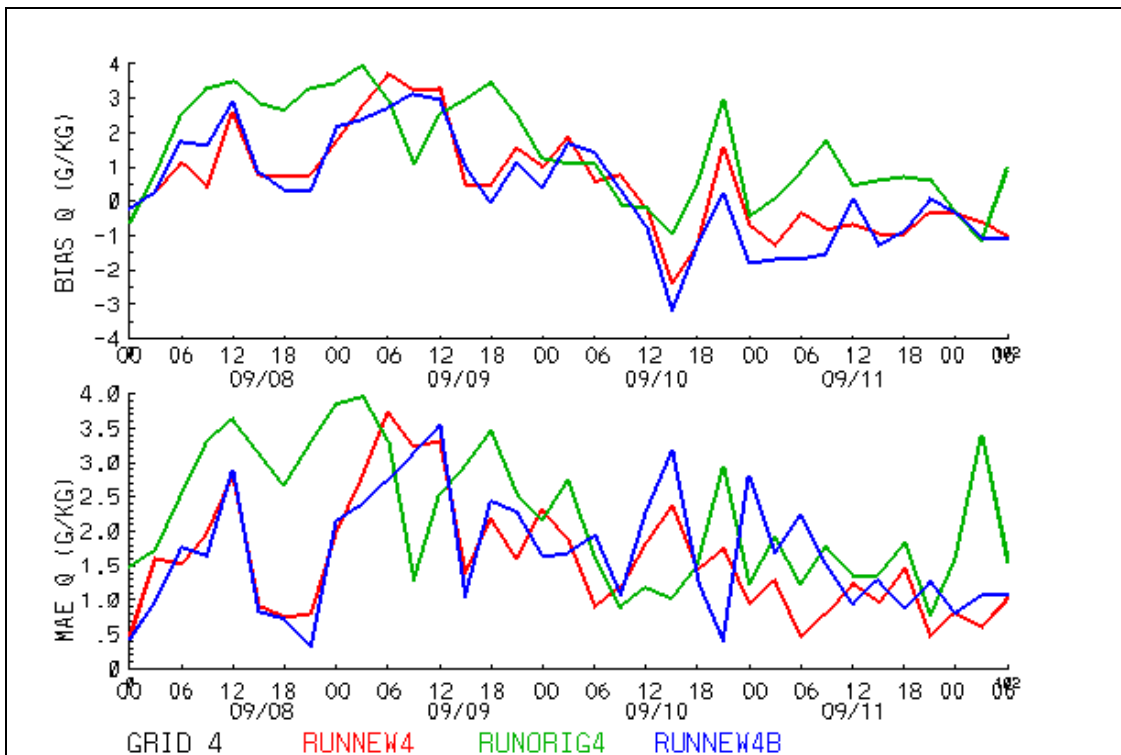


**Figure 47: Specific humidity statistics over domain 4 from 0000 UTC 8 September through 0600 UTC 12 September for the Runnew4 (red line), Runorig4 (green line), and Runnew4b (blue line) simulations.**

## 9. Summary

More than 20 different MM5 simulations were performed in the sensitivity tests completed for this project. These tests investigated the effects of 2, 3, and 4 grids (grid spacings down to 12km, 4 km, and 1.33 km respectively), microphysical parameterizations, PBL parameterizations, and FDDA grid nudging effects. Several points apparent from these experiments are:

- The PBL parameterization has a strong effect on the development (or not) of the thermals and convective cells and should be chosen carefully. Both statistical and qualitative results should be taken into account; the latter including PBL characteristics and frequency of convective cell initiation.
- The choice of microphysical scheme had a secondary effect on the behavior of the model in this case. We do not imply that all cases will be as insensitive to the microphysical schemes. Our focus was on the development of the incorrect convection, not the details of the convection once formed.
- FDDA nudging should be used with caution and understanding.

Resolved convective/thermal development is a consistent theme of these simulations and there is a detailed discussion of this and its relation to non-hydrostatic considerations in Section 7.6. In these simulations, the ETA and Gayno-Seaman PBL schemes both seem to be not mixing heat (and moisture and momentum as well) upwards within the PBL as quickly or efficiently as in the real world. As a result, convective cells form on the lowest

resolvable scale of the model. The grid nudging acts as a filter and forces those cells onto larger scales. We chose the MRF PBL for our final simulations because there was less of a problem with the grid-scale cell development with that scheme, and its PBL heights seemed to be more realistic.

Based on the sensitivity experiments, the MM5 options chosen for the final 5-day 4-grid simulation were

- Kain-Fritsch2 cumulus scheme on grids 1 and 2
- Reisner-1 microphysics
- MRF PBL with  $imvdif=1$  and  $iz0topt=0$
- Soil moisture bucket scheme
- Soil temperature model
- Cloud radiation scheme
- Grid nudging above the PBL.

The results from this simulation were a mixed bag. On the one hand, the results over the primary period of interest, 0000 UTC 8 September through 0000 UTC 9 September, were definitely improved over the results from the previous project. The mesoscale sea breeze developed nicely within the simulation and, on this day, there were not the problems associated with convective cell development seen in the original simulation. However, convective cells did over-develop the next day and persisted throughout the period. A further experiment with the same physics configuration with only three grids (Runnew3) had a more realistic convective development over the period but the minimum grid spacing in that experiment was only 4 km (as compared to 1.3 km in the Runorig4 and Runnew4 simulations). The 3 grid simulation actually performed better statistically than the 4-grid run throughout much of the simulation. We believe that the up-scale concentration and intensification of the convection is a result of the interaction between inadequate PBL processes on the non-hydrostatic scale and the filtering effect of the FDDA. This process is discussed in detail in Section 7.6.

We recommend that the GS scheme should not be used at higher resolution without further testing, both of near-ground effects and also the behavior with resolved convective clouds. Based on our experience with non-hydrostatic models, we also recommend significant basic testing of the MM5 non-hydrostatic scheme itself, especially in simulations where significant non-hydrostatic effects are expected to occur.

There are several additional factors that we did not have time to investigate in this project but should be carefully considered in future work and applications. These include:

- Testing and use of the OSU/NCEP ETA and Pleim-Xu Land Surface Model (LSM) schemes. These schemes are relatively new additions to the MM5 system and require additional inputs not available in the current subset of the NCEP/NCAR Re-analysis data set that we had available. The LSM provides a sophisticated soil moisture and temperature model, snow cover prediction, and vegetation/canopy parameterization. The soil moisture model in the LSM is much more complex than the very simple bucket scheme we used in this project's simulations. The importance of the PBL parameterization has been noted in the above summary - the development of the land surface properties and their interaction with the PBL could be just as important.

- Use of the FDDA grid nudging scheme. The grid nudging parameters should be tested and adjusted for the smaller grid scales used in this project. Because of time constraints, we used defaults in the above nudging simulations. In addition, the analyses that are used in the grid nudging should be examined more closely and the analysis parameters adjusted appropriately.
- Use of the FDDA observation nudging scheme should be considered. As noted in the previous discussion, observation nudging may be more appropriate for smaller scales. However, it is not wise to use the scheme as a black box – many parameters should be tested and adjusted.